Revision 2 (sept 10, 2021) Word Count: 6152

On the occurrence of Jahnsite/Whiteite phases on Mars: a thermodynamic study

Christophe Drouet[a], Matteo Loche[b], Sébastien Fabre[b], Pierre-Yves Meslin[b]

[a]CIRIMAT, Université de Toulouse, CNRS, Toulouse INP, UPS, 4 allée Emile Monso, 31030 Toulouse, France.

[b]Institut de Recherche en Astrophysique et Planétologie, Université de Toulouse, UPS, CNRS, CNES, 9 Avenue du Colonel Roche, 31400 Toulouse, France.

Abstract

Jahnsites/Whiteites are a large family of phosphate hydrate minerals of relevance to Terrestrial and Martian mineralogy. It was recently hypothesized as being present in *Gale Crater* sediments from XRD analyses performed by the *CheMin* analyzer aboard the *Curiosity* rover. However, the conditions of formation and thermodynamic properties of these compounds are essentially unknown to this day. In this work, we have optimized the *ThermAP* predictive thermodynamic approach to the analysis of these phases, allowing us to estimate for the first time the standard formation enthalpy $\Delta H_f°$, Gibbs free energy $\Delta G_f°$ and entropy S° of 15 Jahnsite/Whiteite end-member compositions, as well as of related phases such as Segelerite and Alluaudites. These estimations were then used to feed speciation/phase diagram calculation tools to evaluate the relative ease of formation and stability of these hydrated minerals, including considering present Martian conditions. Selected laboratory experiments confirmed calculation outcomes. All of our data suggest that the formation of Jahnsites is an unlikely process, and

point instead to the formation of other simpler phosphate compounds. The stability domain, as calculated here, also raises serious questions about the possible presence of Jahnsites on Mars as in *Gale Crater*, which appears rather improbable.

Keywords: Jahnsite; Whiteite; Thermochemistry; Phase diagram; ThermAP; PHREEQC; Stability; Curiosity rover; CheMin; Precipitation; Dehydration

Introduction

The terms Jahnsite and Whiteite, as approved by the IMA Commission on New Minerals and Mineral Names, refer to a supergroup of phosphate hydrous compounds, initially described in 1974 from the analysis of the sample $CaMnMg_2Fe_2(PO_4)_4(OH)_2 : 8H_2O$ (Moore and Itô 1974). These minerals share the general formula $XM1M2_2M3_2(PO_4)_4(OH)_2 : 8H_2O$ in which X, M1 and M2 represent mostly divalent cations and where M3 is a trivalent cation in octahedral coordination, dominantly Fe^{3+} for Jahnsites – named after Richard H. Jahns – and Al^{3+} for Whiteites – named after John S. White.

The monoclinic symmetry, space group *P2/a*, was assessed for all samples analyzed. The structure may accommodate a variety of substituting cations, hence the occurrence of several end-member compositions (often involving manganese)(Grey et al. 2020) and possibly solid solutions. Among reported substituting elements are Ca^{2+}, Mn^{2+}, Na^{+} in X sites, Mg^{2+}, Mn^{2+}, Fe^{2+} or Fe^{3+} in M1 sites and Mg^{2+}, Mn^{2+}, Fe^{2+} (Fe^{3+}) or Zn^{2+} in M2 sites. While M1 and M2 involve divalent cations again in 6-fold octahedral coordination, X ions are located in 8-fold cages formed by adjacent phosphate oxygens. As a general observed trend, although exceptions may occur, the cations radii tend to follow an increasing tendency in the order M3 < M2 < M1 < X (Kampf et al. 2019). The crystal structure (**Figure 1**) of several end-member compositions has been explored in detail, from the analysis of specimens from different terrestrial origins: **Table 1** reports the main members of the Jahnsite and Whiteite subgroups known to date, along with typical localities where they were observed. Additional information on localities containing Jahnsites or Whiteites may be found for example in the MinDat.org online database, respectively with references No. 53039 and 29343. Although these compounds do not represent a high volumetric proportion of phosphate minerals on Earth (Treiman et al. 2021), they were nonetheless observed punctually at distinct places on several continents.

In spite of the above, the conditions of formation of Jahnsites/Whiteites remain highly unclear. No reports have been made available, to the best of our knowledge, neither on the preparation of pure Jahnsite/Whiteite synthetic analogs in view of systematic crystallization or dissolution studies, nor on the exploration of their thermodynamic properties (e.g. via calorimetry approaches), which remain essentially unknown. Only a single report addressed the thermal decomposition of one Jahnsite-(CaMnMn) and one Whiteite-(CaMnMg) specimen, pointing to a degradation pattern until complete dehydration/dehydroxylation (Grice, Dunn, and Ramik 1990). For the Jahnsite-(CaMnMn) compound, the authors mentioned an Alluaudite-like X-ray diffraction (XRD) pattern without further details. Unveiling the energetics of Jahnsites (in iron-rich contexts) and Whiteites (aluminum-rich) versus their chemical composition would allow understanding further their conditions of formation and exploring their related stability fields depending on local environmental constraints (past or present), not only on Earth but also in other contexts such as the surface of Mars.

Very recently, these phases have attracted attention as they were suspected, for the first time, to be potentially present on Mars, from XRD analyses carried out in the *Glen Torridon* area of *Gale Crater*, by the *CheMin* onboard instrument of the *Curiosity* rover (Treiman et al. 2021). Based on XRD data, a remarkable sharp peak corresponding to a *d*-spacing of ~9.22 Å, not easily assignable to other rock-forming minerals, was indeed detected and potentially assigned to the presence of Jahnsites/Whiteites. According to the authors of this communication, "*it is conceivable that they could also form during diagenesis on Mars. There is ample evidence for diagenesis in the Murray formation mudstones, including mobility and recrystallization of iron oxides on Vera Rubin Ridge and formation of Mn-rich nodules in Glen Torridon. For the environments of Glen Torridon rocks, Jahnsite-Whiteite group minerals could have formed during low-temperature alteration of apatite by acid sulfate solutions rich in Mn (and possibly Fe). It is not clear why Jahnsite-Whiteite might be present alone, without detections of any other secondary phosphate minerals*". In addition, the dark polygonal objects analyzed by *CheMin* point to an enrichment

in Mn "*which (by its several valence states) can serve as an energy source for chemosynthetic microorganisms*" (Treiman et al. 2021); and the search for signs of Martian life has clearly been identified as an objective for the current/future investigations of Mars surface – e.g. via the Perseverance rover (landed on February 2021).

On Earth, Jahnsites/Whiteites are suspected to form by alteration of primary iron and/or manganese phosphates as in granitic pegmatites (Moore and Araki 1974; Kampf et al. 2018; Grey et al. 2010). They were reported as "*late-stage hydrothermal products of the decomposition of triphylite-lithiophilitein pegmatites [occurring] in a paragenesis with laueite, strunzite, and stewartite*" (Moore and Araki 1974). Their formation was suggested to have occurred in solution at low temperature (Moore and Itô 1974). Another related hydrous mineral seems to be Segelerite $CaMgFe^{III}(PO_4)_2OH : 4H_2O$ whose thermochemistry is not known either. These phases have also been, at times, observed in sedimentary deposits (Elliott and Willis 2019). It may also be noted that Jahnsites have also been described in totally different settings, as in the composition of urinary stones, although on rare occasions (Abboud 2008).

Whether for Terrestrial or Martian investigations, better apprehending the thermodynamic properties of Mn-bearing phosphates such as Jahnsites and Whiteites is crucial in view of assessing their stability domains or proposing/explaining evolution trends. In particular, it may help to critically discuss the hypothesis of their presence on Mars, which is the purpose of this contribution. Since no experimental data are available to assess directly the thermodynamic properties of these compounds, we expanded here the "Applied Predictive Thermodynamics" model *ThermAP* (Drouet and Alphonse 2015) to such phases. This model was previously set up and applied successfully to the phosphate apatite group of minerals (Drouet 2015, 2019). To this aim, the model was based here on known thermodynamic data from a series of related mineral compounds (generally phosphates) involving ions relevant to the Jahnsite/Whiteite system and included in the *Thermoddem* mineralogical database, allowing calculations with speciation programs such as PHREEQC. Finally, based on our thermodynamic considerations and

This is the peer-reviewed, final accepted version for American Mineralogist, published by the Mineralogical Society of America.
The published version is subject to change. Cite as Authors (Year) Title. American Mineralogist, in press.
DOI: https://doi.org/10.2138/am-2022-8174. http://www.minsocam.org/

Mars mineralogy around the *Gale Crater*, illustrative stability assessments will be made and the eventuality of presence of such phases on Mars will be discussed.

Materials and Methods

ThermAP predictive thermodynamic calculations for minerals

ThermAP is a predictive calculation tool aiming to estimate the standard properties of complex oxides (at 298 K and 1 bar) from a linear combination of the corresponding properties for constitutive simple oxides. Typical outcomes of the program are the standard formation enthalpy $\Delta H_f°$ and Gibbs free energy $\Delta G_f°$, from the elements taken in their standard state, as well as the standard entropy S° of the complex oxide. For example, $\Delta G_f°$ of a complex oxide can be decomposed, in *ThermAP*, as follows:

$$\Delta G_f°(complex\ oxide) = \sum_i v_i \cdot g_i = \sum_i v_i \cdot \left(a_{corr,G_i} \cdot \Delta G_f°(binary\ oxide)\right) \quad \textbf{Eq. 1}$$

where v_i denotes the stoichiometric coefficient for ion *i* in the chemical formula, g_i is the Gibbs free energy contribution of this ion, and $a_{corr,Gi}$ is a corrective factor applicable to the simplest oxide formed with ion *i* (for halides, the diatomic molecule is taken as reference). This approach, inspired from other works on predictive thermodynamics (e.g., La Iglesia 2009) but further investigated, has been particularly developed so far in the illustrative case of phosphate apatites and led to $\Delta G_f°$, $\Delta H_f°$ and S° estimates generally within 0.5 to 1% of relative error (Drouet 2019, 2015). For simplification of use, in the *ThermAP* formalism, each ion in the chemical formula is associated with a triplet (g_i, h_i, s_i) denoting their Gibbs free energy, enthalpy and entropy contributions; keeping however in mind that it originally refers to the corresponding simple oxide. For instance, values assigned as g_{Ca}^{2+} and g_{PO4}^{3-} correspond respectively to $\Delta G_f°(CaO)$ and $½ \cdot \Delta G_f°(P_2O_5)$ to which corrective factors are associated to consider the

121 complex oxide characteristics. The core of this approach is the determination of the corrective factors,
122 which are expected to differ from one subfamily of compounds to another. These factors were shown to
123 be directly related to physicochemical characteristics of the elements considered, e.g. in terms of
124 electronegativity (Drouet 2019, 2015).
125 In practice, the corrective factors to apply for a given family of compounds are accessed by multiple
126 iterations (ion by ion) comparing the *ThermAP*-calculated values of $\Delta G_f°$, $\Delta H_f°$ or S° to data accessible as
127 "reference" in the literature. However, when no reference data are available, as is the case of Jahnsites
128 and Whiteites, it remains possible to consider a subpopulation of related solid phases sharing similar
129 compositional features (Drouet 2019). The 23 phosphate phases taken into account in the present work
130 for assessing the (g_i, h_i, s_i) values to apply to Jahnsites/Whiteites are listed in **Table S1** (Supporting
131 Information); they were selected on the basis of their chemical composition involving ions relevant to
132 Jahnsites/Whiteites (essentially based on **Table 1**) and for their known thermodynamic properties,
133 including in the extensive and updated *Thermoddem* database of mineral phases (Blanc et al. 2012)
134 usable in PHREEQC calculations.
135

136 **PHREEQC speciation/phase predominance calculations**

137 PHREEQC is a computer program for geochemical modeling in aqueous conditions, developed by the US
138 Geological Survey (Parkhurst and Appelo 2013). It can perform a wide variety of calculations such as
139 speciation, equilibrium between gas, solid and aqueous solution, reactions of dissolution and
140 precipitation, and calculation of saturation index (SI). Calculations are based on the chemical properties
141 of dissolved species, solids and gases from a given database, and can be performed over a quite large
142 range of temperatures and pressures, provided that T-/P-specific data are available (Appelo, Parkhurst,
143 and Post 2014). Here, we have used the *Thermoddem* database (Blanc et al. 2012), developed by the
144 French geological survey, Bureau de Recherches Géologiques et Minières (BRGM). We selected this

database for the wide variety of solid species, including numerous secondary minerals with phosphorus, and for the regular update it receives, making it a solid base to perform geochemical modeling. Some of the database properties were verified by the *ThermAP* software (see below) allowing us to implement Jahnsite-Whiteite mineral, make punctual corrections for some minerals and confirm the solidity of the database. In addition, we used PHREEPLOT, a program with an embedded version of PHREEQC, to generate multiple plots to create predominance phase diagrams (Kinniburgh and Cooper 2011).

For these calculations, the effective parameter used was log K, where K represents the solubility product of the considered solid phase (considering the speciation $H_2PO_4^-{}_{(aq)}$ for aqueous phosphate ions). By definition of the solubility product, log K is directly related to the change in Gibbs free energy of the dissolution reaction, ΔG_{disso}, itself being linked to the Gibbs free energy of formation of the given phase as follows:

$$\Delta G_{disso}(Jahnsite) = \Delta G°_{disso}(Jahnsite) + 2.3\ RT\ log\ K = 0\ (solubility\ equilibrium) \quad \textbf{Eq. 2}$$

$$\Delta G°_{disso}(Jahnsite) = -2.3\ RT\ log\ K = \Delta G_f°(Jahnsite) - \sum_{elements} v_{element}\ \Delta G_f°(element) \quad \textbf{Eq. 3}$$

Calculations were made firstly by considering selected amounts of starting salts to dissolve, temperature (typically 100°C) and stoichiometry ratio, to mimic laboratory experiments run in this study. In particular, we worked here essentially with the Ca-Mn^{II}-Mg-Fe^{III}-P-O-H system, aiming the formation of the "historical" Jahnsite-(CaMnMg) compound $CaMnMg_2Fe_2(PO_4)_4(OH)_2 : 8H_2O$ (Moore and Araki 1974).

In a first stage, calculations were made starting from a stoichiometric mixture of precursor salts involving the ions in question here. Selected starting salts were those accessible for laboratory experiments and involving counter-ions such as nitrates or chlorides instead of sulfates for limiting the precipitation of undesirable secondary phases: $Ca(NO_3)_2 : 4H_2O$, $MnCl_2 : 4H_2O$, $Mg(NO_3)_2 : 6H_2O$, $FeCl_3 : 6H_2O$ and KH_2PO_4. With this modeled replication of experiments, a predominance diagram for the solid and dissolved species in the Log $f(O_2)$/pH space was generated. Then, the salts are allowed to dissolve in pure water,

and activities of typically phosphorus, manganese, iron, magnesium and calcium species are derived. When SI > 0 for a given solid, supersaturation is reached, meaning it is thermodynamically possible to precipitate it from the solution. Several minerals can reach supersaturation, but not all of them will precipitate because of the difference between kinetic rates for example. Finally, we authorized precipitation of the saturated minerals, targeting the same results as the predominance diagram, in addition to eventual secondary predominant species or minerals. Even though the kinetics of precipitation is not accounted for in such calculations, this method can show how likely it is to supersaturate species such as Jahnsite/Whiteite in our assumed favorable experimental conditions.

After the modeled replication of potential laboratory experiments, we applied the same methods for the ancient Mars conditions to assess the possibility of forming Jahnsite/Whiteite using our modeled alteration solution assuming that P and Mn were mobile and available at the same time as dissolved species in the solution.

Laboratory precipitation experiments

Selected laboratory experiments were run starting from stoichiometric proportions corresponding to the "historical" Jahnsite-(CaMnMg) $CaMnMg_2Fe_2(PO_4)_4(OH)_2 : 8H_2O$ that gathers relevant ions for both Terrestrial and Martian contexts. The precursor powders used are as follows: $Ca(NO_3)_2 : 4H_2O$ (typically 708.45 mg), $MnCl_2 : 4H_2O$ (593.7 mg), $Mg(NO_3)_2 : 6H_2O$ (1538.46 mg), $FeCl_3 : 6H_2O$ (1621.8 mg) and KH_2PO_4 (1633.08 mg), involving counter-ions such as nitrates or chlorides instead of sulfates for limiting the precipitation of undesirable sulfated or chlorinated secondary phases. After preliminary dissolution of each salt separately in about 1.5 to 2 ml, all precursor solutions were rapidly mixed together and the total volume was adjusted to 10 ml. In some experiments, the natural pH of the obtained medium was left unaltered, typically around 0.4 (which is close to the pH used in other studies as for the precipitation of Jarosites to avoid iron III hydrolysis, (Drouet and Navrotsky 2003)). In other trials, up to +10 ml of a

This is the peer-reviewed, final accepted version for American Mineralogist, published by the Mineralogical Society of America.
The published version is subject to change. Cite as Authors (Year) Title. American Mineralogist, in press.
DOI: https://doi.org/10.2138/am-2022-8174. http://www.minsocam.org/

concentrated solution of potassium hydroxide KOH (pH ~ 13) were progressively added to the medium to increase the amount of OH^- ions. After mixing the precursors, the precipitating medium was left to mature for about 24 hours, either at room temperature (about 20 °C) or 60°C or 100 °C prior to filtration, washing with deionized water and drying in an oven preset to 40 °C. The obtained precipitates were analyzed by X-ray diffraction (XRD) with an Equinox 100 INEL curved-counter diffractometer powered at 30 kV / 30 mA and using a cobalt anticathode (λ_{Co} = 1.78892 Å) with an acquisition time of ~ 1 hour per sample. XRD patterns were examined with the *Match* software exploiting the PDF-2 database.

Results

Development of the *ThermAP* model for Jahnsites/Whiteites

Gibbs free energy. With the view to ultimately run phase predominance calculations – for example via the PHREEQC software – and also because it embodies the thermodynamic driving force in a reaction or cycle, we chose to consider first the Gibbs free energy $\Delta G_f°$, and thus the related log K values, as the parameter to be fitted first. We selected here a subpopulation of 23 phosphate minerals (listed on **Table S1**) involving relevant ions to Jahnsites/Whiteites. This allowed us to determine the g_i ionic contributions leading, for this subpopulation of compounds, to the best fit between calculated and reference data (using the *Thermoddem* database), and these values are reported on **Table 2** (second column).

Figure 2 shows the comparison between calculated and reference $\Delta G_f°$ values for the phases considered here, illustrating as expected the good match throughout this series of solid phases, with a mean relative error of 0.6 % (in absolute value). Note that for three phases the values of $\Delta G_f°$ compiled in *Thermoddem* were found somewhat different from other literature data: Vivianite $Fe_3(PO_4)_2 : 8\ H_2O$, magnesium hydrogen phosphate $MgHPO_4$ and calcium aluminum phosphate $CaAlH(PO_4)_2 : 6H_2O$. For these phases,

the reference values listed by Vieillard and Tardy were selected instead, see **Table S2** (Vieillard and Tardy 1984). The corresponding graph in terms of log K is shown in **Figure S1**. Although the calculation process to access log K from $\Delta G_f°$ involves several steps so as to consider the whole dissolution reaction, and thus further propagates uncertainties, there is still an appreciably good correspondence between calculated and reference data.

Entropy. Previous developments of the *ThermAP* approach on apatites showed that determining $\Delta H_f°$ from $\Delta G_f°$ and S° led to a better overall fit (especially for S° values) than drawing S° from $\Delta G_f°$ and $\Delta H_f°$ due to a difference in propagated uncertainties (Drouet 2015). Therefore, we also selected this methodology here and S° was thus considered as the second parameter to be fitted, after $\Delta G_f°$.

Only few values of S° are however available in the literature concerning the 23 phases relevant to this study. For phases with missing entropy data, we evaluated S° using Helgeson's method by considering theoretical equilibria involving only solid phases (Helgeson 1978). This method is quite common for the estimation of entropies of solids, and is based on the idea that the volume change along solid-state reactions remains very small, thus suggesting an entropy change ΔS of reaction also close to zero. Therefore, by assuming that the sum of entropies of the left members of the reaction equals that of the right members, it becomes possible to access the unknown S° term. An example may be given in the case of $FePO_4 : 2H_2O$ (Strengite or Phosphosiderite) for which the following theoretical reaction in solid state may be written:

$$FePO_4{:}\,2H_2O + Al(OH)_3 \leftrightarrow \ AlPO_4{:}\,2H_2O \ + Fe(OH)_3 \qquad \textbf{Eq. 4}$$

From the S° values of Variscite ($AlPO_4 : 2H_2O$), aluminum and iron III hydroxides, respectively equal to 134.5 (Vieillard and Tardy 1984), 71.128 (Barin 1995a) and 106.7 (Barin 1995b) $J.mol^{-1}.K^{-1}$, one can estimate $S°(FePO_4 : 2H_2O) \cong 170.1$, which is very close to the reference value of 171.25 $J.mol^{-1}.K^{-1}$

(Vieillard and Tardy 1984), within 0.7 % of relative error in this case. The solid-state reactions considered in this work for phosphate phases with missing entropy data are listed in **Table S3**.

Then, via multiple iterations as was done above for g_i, the ionic entropy contributions si were determined by seeking the best fit between *ThermAP*-calculated S° values and "reference" ones (i.e. whether taken from the literature or accessed here by Helgeson's method). These s_i values are also listed in **Table 2** and **Figure 3** shows the comparison between these two sets of data. Again, a general good match was obtained, with a mean relative error of 3.3 %.

Enthalpy. From the fits obtained above in terms of Gibbs free energy and entropy, it then became possible to draw enthalpy contributions for the 23 phosphate phases of interest here, using the general formula:

$$\Delta H_f^\circ = \Delta G_f^\circ + T \cdot \Delta S_f^\circ \qquad \textbf{Eq. 5}$$

with T = 298 K in the present case and where ΔS_f° refers to the entropy of formation of the considered phase from the elements in their standard state.

Fitting via *ThermAP* the obtained ΔH_f° values as was done earlier for g_i and s_i then allowed us to determine the ionic contributions h_i that were added to **Table 2**. Note that it is also possible to reach these same h_i values from the ionic contributions g_i and s_i. However, it is then important to keep in mind that while h_i and g_i denote changes in enthalpy and free energy from the elements composing the corresponding simple oxide, in contrast s_i refers directly (as is customary) to the sole standard entropy. Therefore, strictly speaking, the following relation applies:

$$h_i = g_i + T \cdot \left(s_i - \sum_{\substack{elements\ from \\ simple\ oxide}} S^\circ_{elements} \right) \qquad \textbf{Eq. 6}$$

The comparison between the calculated $\Delta H_f°$ values obtained and reference data, when available, is shown in **Figure 4**. Again, a very good agreement is obtained between the two sets of data (mean relative error 0.2 %) when existing reference values are accessible.

Recommended thermodynamic properties for Jahnsites/Whiteites

The above findings allowed us to determine ionic energetic contributions in terms of Gibbs free energy (and related log K), enthalpy and entropy for 23 phosphate minerals comprising ions most relevant to the composition of Jahnsites and Whiteites, namely Ca^{2+}, Mg^{2+}, Mn^{2+}, Fe^{2+}, Fe^{3+}, Al^{3+}, PO_4^{3-}, OH^- (see **Table 2**). Hydration H_2O was also included as fitted chemical species, along with secondary ions like H^+ and F^-, which were present in some of the minerals considered. Some other ions have also occasionally been reported in the composition of Jahnsites, such as Na^+ and Zn^{2+}. The energetic contributions of these cations were thus also calculated (based on phases listed in **Table S1**) and added to **Table 2**, along with those of potassium, another relatively common cation in minerals (e.g. as in Leucophosphite $KFe^{III}_2(OH)(H_2O)(PO_4)_2 : H_2O$), in case this ion may happen to be involved in further Jahnsite/Whiteite samples yet to discover.

Based on this *ThermAP* development for related phosphate phases, it then becomes possible to propose thermodynamic predictions for Jahnsites/Whiteites at 298 K / 1bar depending on their chemical composition. Taking into account the main end-members listed in **Table 1**, the corresponding values of $\Delta G_f°$, $\Delta H_f°$, S° and log K (dissolution constant using the $H_2PO_4^-$ phosphate speciation) have for example been calculated, at 298 K and 1 bar, and gathered in **Table 3**. To the best of our knowledge, these are the first thermodynamic estimates reported for Jahnsites and Whiteites compounds.

From the *ThermAP* refined values of g_i, h_i, s_i tabulated in **Table 2**, it is also possible to draw estimates of any envisioned solid solutions within the Jahnsite/Whiteite system. For instance, the calculation of $\Delta G_f°$

for Jahnsite-(NaMnMn) reported from Quarry, Australia (Miyawaki et al. 2019), whose actual chemical formula was reported as $NaMn(MnFe^{III})Fe^{III}_2(PO_4)_4(OH)_2 : 8H_2O$ (see **Table 1**) yields -7695 kJ/mol. Besides solid solutions, departure from stoichiometry and/or from the theoretical $8H_2O$ hydration may also be accounted for in the *ThermAP* approach (as was shown for example previously on apatites (Drouet 2015)). These refined (g_i, h_i, s_i) sets of ionic contributions for Jahnsites and Whiteites have now been added to the *ThermAP* program accessible from the internet (freely available to the scientific community, Drouet and Alphonse 2015).

We may also remark that no thermodynamic data appears to be available in the literature for related phosphate phases such as Segelerite $CaMgFe^{III}(PO_4)_2OH : 4H_2O$ (orthorhombic, *Pcca* space group). In a similar way as was done for Jahnsites, the thermodynamic properties $\Delta G_f°$, $\Delta H_f°$, $S°$ and log K at 298 K may be estimated using the g_i, h_i, s_i values refined here (see **Table S4**). Alluaudites are another family of phosphate minerals involving similar types of ions as Jahnsites and belonging to the general formula $A1A2M1M2_2(PO_4)_3$ although having large departures from this theoretical formula in terms of site occupations (e.g., Alhakmi et al. 2018). Additionally, Grice *et al.* (1990) reported that an Alluaudite phase formed upon Jahnsite dehydration (Grice, Dunn, and Ramik 1990). Based on the Jahnsite-(CaMnMn) composition studied by these authors, it is possible to assume the chemical composition of the Alluaudite phase obtained (not detailed in this referenced paper) by writing the decomposition pattern:

$$CaMnMn_2Fe_2(PO_4)_4(OH)_2 : 8H_2O \rightarrow 4/3\ Ca_{0.75}Mn_{0.75}Mn_{0.75}Fe^{III}_{1.50}(PO_4)_3 + MnO + 9\ H_2O_{(gas)} \quad \textbf{Eq. 7}$$

and the thermodynamic properties of this Alluaudite "$CaMnMnFe^{III}$" may then be estimated with our *ThermAP* refinement as well (added to **Table S4**). Note indeed that exsolution of some Mn^{2+} ions into MnO as a secondary phase is more thermodynamically favored than exsolution of Ca^{2+} into CaO, as

suggested by the smaller value of $\Delta G°$ of reaction (that we can calculate to 151 kJ/mol versus 215 kJ/mol). If a similar dehydration pattern into an Alluaudite phase is also valid for other Jahnsites, then similar calculations can be made on the basis of their chemical compositions. For example, it may be suggested that the "historical" Jahnsite-(CaMnMg) would lead to an Alluaudite "CaMnMgFe" whose composition and *ThermAP*-calculated thermodynamic properties have been added to **Table S4**.

In all these calculations, it is difficult to state the absolute error being made since no experimental thermodynamic data are available on these complex phases. However, as shown during the *ThermAP* refinement in this work, the $\Delta G_f°$, $\Delta H_f°$ and S° values for the 23 phosphate phases used in the refinement were systematically close to the experimental reference data, typically within 0.6 % of relative error for Gibbs free energies, 0.2 % for enthalpies and 3.3 % for entropy (keeping in mind that the entropy contribution $T \cdot \Delta S_f°$ for such complex oxides, high large ionic contents remains usually significantly lower than the enthalpy contribution $\Delta H_f°$ in the calculation of $\Delta G_f°$). Therefore, we can consider reasonably – as was found previously on apatite phosphates (Drouet 2015) – that the $\Delta G_f°$, $\Delta H_f°$ and S° values recommended here for Jahnsites/Whiteites (**Table 3**) and related phases probably stand within about 1 % of relative error.

Speciation/phase predominance calculations

Now that estimates of the thermodynamic properties for the formation of Jahnsite/Whiteite phases have become available via *ThermAP*, it is possible to add these phases in the database of speciation/phase predominance programs so as to run phase speciation/predominance calculations. We have here selected the PHREEQC / PHREEPLOT software to this aim, and added the Jahnsite/Whiteite phases to the *Thermoddem* database. In particular, we selected the Ca-Mn^{II}-Mg-Fe^{III}-P-O-H system, aiming the formation of the "historical" Jahnsite-(CaMnMg) compound $CaMnMg_2Fe_2(PO_4)_4(OH)_2 : 8H_2O$

(Moore and Araki 1974), involving ions particularly relevant to putative phosphate phases observed in *Gale Crater*.

Calculations were made considering a stoichiometric mixture Ca-Mn-Mg-Fe-P of precursor salts. Although these calculations cannot take into account kinetic factors, this approach can illustrate how likely it is to supersaturate Jahnsite in our assumed favorable experimental conditions. First, the saturation index SI versus relevant phases was calculated, whether in equilibrium with or isolated from the Terrestrial atmosphere (to mimic potential laboratory experiments) as shown in **Figure 5a**. Several phases exhibit a significantly positive SI value such as Hematite Fe_2O_3, Strengite $FePO_4 : 2H_2O$, Lepidocrocite/Goethite FeO(OH) or manganese hydrogen phosphate $MnHPO_4$. In this scheme, Jahnsite on the contrary only appears very minor. Then, precipitation of phases was allowed in the software, unveiling Strengite and potentially $MnHPO_4$ as the most probable final products (**Figure 5b**).

In addition, predominance diagrams for solid and dissolved species were calculated using the whole Thermoddem database and plotted using PHREEPLOT, in the Log $f(O_2)$/pH space (**Figure 6**). These diagrams show predominance domains for the cationic elements involved in the composition of Jahnsite, namely Ca^{2+}, Mn^{2+}, Fe^{3+} and Mg^{2+}, starting from concentrations and elemental ratios similar to **Figure 5**. We can infer that Jahnsite precipitation never occurred in any of our phase diagram calculations.

Laboratory precipitation experiments

To complement our calculations, selected laboratory experiments were run in the same stoichiometric conditions as for the above PHREEQC calculations, focusing on the precipitation of the "historical" Jahnsite-(CaMnMg). In order to allow the initial dissolved salts to react, and to attain thermodynamic equilibrium faster, a reference experiment was run at 100°C for 24 hours without external alteration of pH (initial pH measured to ~ 0.4). Pictures of the obtained precipitate after thorough washing are shown

for illustrative purpose in **Figure S2**. The XRD pattern obtained by analyzing the precipitate (**Figure 7**) clearly demonstrated the presence of iron III phosphate dehydrate $FePO_4 : 2H_2O$ as essential constituent (sum of the two polymorphs Strengite and Phosphosiderite). These results are in accordance with our PHREEQC calculations pointing to $FePO_4 : 2H_2O$ as the predominant expected compound. The co-presence of secondary phases containing Mn remains possible, either as minor crystalline phase(s) or amorphous, or else via Mn^{2+} doping into the iron phosphates. The purplish color of the precipitate suggests indeed the presence of this element within the sample despite non-specific XRD peaks. The absence of Jahnsite appears however quite clearly by the absence of any detectable XRD feature around $2\theta \sim 11°$ ($\lambda_{K\alpha}$ cobalt anticathode) corresponding to the typical Jahnsite d-spacing at ~ 9.22 Å (most intense peak in the Jahnsite pattern, see Power Diffraction File (PDF) 01-070-2079). Despite the stoichiometric initial elemental ratios corresponding strictly to the composition of Jahnsite-(CaMnMg), namely $CaMnMg_2Fe_2(PO_4)_4(OH)_2 : 8H_2O$, and despite supersaturation conditions with respect to this phase (**Figure 5a**), it did not precipitate experimentally.

Variations of the precipitation conditions were also tested in terms of maturation temperature (by lowering the maturation temperature to potentially facilitate the precipitation of hydrated phases such as Jahnsites) and/or via the addition of an alkaline solution of potassium hydroxide (so as to add OH^- ions to the medium and potentially facilitate the formation of Jahnsite which is a hydroxy-phosphate compound). The modification of the maturation temperature from 100 °C down to 60 or 20 °C, however did not result in precipitation of Jahnsite. At 60 °C, the analysis of the precipitate by XRD (**Figure S3a**) showed the formation of iron III phosphate in the form $H_3Fe(PO_4)_2 : 2.5H_2O$ (PDF 00-044-0812) – which may be seen as a hydrated precursor to Strengite/Phosphosiderite – in addition to a remaining amorphous phase. At 20 °C, only a minor amount of precipitate was observed at 24 hours. Therefore, lowering the temperature probably essentially affected the kinetics of evolution of the precipitate, but Jahnsite was never detected. The addition of KOH, even if dropwise and independent of the maturation

375 temperature, instantly led to the formation of a brownish precipitate while the supernatant overall pH
376 did not rise. These observations suggest the immediate combination of the added OH^- ions with ionic
377 species to form OH-bearing phases. Analysis by XRD (**Figure S3b**) evidenced the amorphous nature of this
378 precipitate, as only halos were observable around 2θ = 33° (major) and 16° (secondary). No crystallized
379 phase formed at these conditions.

380

381 **Discussion**

382 Jahnsites/Whiteites constitute a large family of phosphate hydrated minerals sharing the same global
383 structure (**Figure 1**). These phases were observed on Earth on several places/continents (**Table 1**),
384 although they only represent a small volumetric portion of phosphate minerals. Recently, they have
385 been suspected to be present on the surface of Mars, based on an XRD peak noticed at ~9.22 Å by the
386 *CheMin* apparatus aboard the rover *Curiosity* while analyzing samples from the *Glen Torridon* area of
387 *Gale Crater*, containing dark-toned nodules whose chemical analyses indicated the concomitant
388 presence of manganese and phosphorus (Treiman et al. 2021; Lanza et al. 2021). However, to this day,
389 their conditions of formation and thermodynamic properties remain totally unknown. To shed light on
390 these aspects, and potentially favor or disfavor the hypothesis of their presence on Mars, we have
391 expanded in this study the *ThermAP* predictive thermodynamic approach to the case of these
392 compounds. Comparisons between theoretical and calculated values on 23 related phosphate mineral
393 phases involving ions relevant to Jahnsites/Whiteites, shown in Figs 2,3,4, indicate a very good match.
394 Optimization of *ThermAP* to this subpopulation of compounds thus allowed us to ultimately derive the
395 ionic enthalpy, Gibbs free energy and entropy contributions, respectively h_i, g_i and s_i (**Table 2**) to apply to
396 the chemical formula of any given Jahnsite/Whiteite phase so as to estimate their $\Delta G_f°$, S° and $\Delta H_f°$ and

log K properties, at 298 K and 1bar – typically within about 1 % of relative error. Hence, the values that we recommend in this work for the end-members listed in **Table 1** are given in **Table 3**.

Thanks to these estimations, and in particular of ΔG_f° and the related log K values, it then became possible to add these data to thermodynamic databases in order to run speciation/phase diagrams. We selected the PHREEQC software and the *Thermoddem* database for their robustness, relevance to the mineralogy field and regular updates. Our speciation calculations (**Figure 5**) considering the "historical" Jahnsite-(CaMnMg) strongly suggest that it is not a favorable phase expected to precipitate even in potentially advantageous conditions such as stoichiometric proportions in the initial solution, while other compounds such as $FePO_4 : 2H_2O$ (e.g. Strengite) or $MnHPO_4$ clearly appear as preferential phases. Temperature and pH did not affect our results significantly. Although kinetic factors are not accounted for in such calculations, it allows identifying which mineral phase should more likely precipitate. Our mimicking laboratory experiments starting from stoichiometric conditions indeed pointed out from XRD analyses the absence of a Jahnsite phase in the precipitate and revealed the formation of $FePO_4 : 2H_2O$ as crystalline phase (**Figure 7**). Phase predominance diagrams considering one by one each type of cation involved in the composition of Jahnsite-(CaMnMg) were also plotted (**Figure 6**). Again, Jahnsite did not appear as a favorable phase to be formed.

Implications

The results reported in this work can be applied to current and past Martian conditions to question the possible occurrence of Jahnsite in *Gale Crater*. As expected, our calculations for different CO_2 pressures (~6 mbars for present-day Mars and ~500 mbars for ancient Mars (Kurokawa, Kurosawa, and Usui 2018)) did not change the predominance diagrams (**Figure 6)** significantly and exclude the formation of Jahnsite under these conditions. In terms of oxygen fugacity, the present-day Martian conditions (log $f(O_2)$ = -5.02

(Trainer et al. 2019)) correspond to the upper part of the diagrams in **Figure 6** and do not appear to favor Jahnsite precipitation either. Although the past *f(*O2) is unknown, these diagrams cover a very wide range of fugacities, ruling out an effect of this parameter on Jahnsite formation.

The solution used to obtain these diagrams is thermodynamically favorable for Jahnsite precipitation, with elemental stoichiometric proportions and high concentrations of its constituents. Since weathering fluids under ancient Martian conditions are not expected to contain such elevated concentrations of these elements (Bridges et al. 2015), direct Jahnsite precipitation was very unlikely.

Even though Jahnsite had formed by other indirect pathways, our model also allows investigating its stability under present-day Mars conditions. The single literature report dealing with the thermal degradation of Jahnsite-(CaMnMn) showed a start of degradation at a quite low temperature, with a first peak maximum at 125 ° C, and the formation of an Alluaudite phase after complete dehydration/dehydroxylation (Grice, Dunn, and Ramik 1990). Considering this observation and the *ThermAP*-derived thermodynamic properties of Jahnsites and Alluaudites (see **Table S4**), including their anticipated temperature dependence based on isobaric heat capacity C_p considerations (**Table S5**), it is possible to plot stability curves of the Jahnsite-Alluaudite system in the $f(H_2O)$-T space, as was done previously on Jarosites on *Meridiani Planum* (Navrotsky, Forray, and Drouet 2005) – where $f(H_2O)$ denotes water fugacity. **Figure 8** illustrates the example of three Jahnsites (CaMnMn), (CaMnMg) and (MnMnMg). These phases were chosen because they cover compositions relevant to *in situ* observations (Treiman et al., 2021; Lanza et al., 2021). As water fugacity drops, the stability temperature significantly decreases, reaching negative values for Log $f(H_2O)$ lower than -4, i.e., under 0.1 mbar. Taking into account the "typical" low water vapor on the present Martian atmosphere in *Gale crater*, e.g. ~ $0.5 . 10^{-3}$ mbar (Log $f(H_2O)$ = -6.3 (McConnochie et al. 2018)), these findings suggest that Jahnsite dehydration is expected to occur above -43 °C for Jahnsite-(CaMnMn) and above -47 °C for Jahnsites-(CaMnMg) and (MnMnMg). The ground temperature at *Gale Crater* was measured by *Curiosity* to range from

444 -93°C and to10°C (Vasavada et al. 2017). Under these conditions, Jahnsites present at the surface of Mars
445 would regularly encounter periods of unstable conditions leading to their progressive dehydration.

446 All of our data unanimously suggest that Jahnsites are not favorable phases to precipitate directly, even
447 starting from a stoichiometric mixtures, and that other phases should probably be expected to form
448 instead, e.g. more simple phases such as iron phosphate dehydrate or $MnHPO_4$. Extrapolation of our
449 results to present and past Martian conditions, which are even less favorable than our laboratory and
450 numerical experiments, also argues against their direct precipitation at the surface of Mars. Moreover,
451 any Jahnsite formed by other indirect pathways and brought to or formed at the surface of Mars would
452 undergo a progressive dehydration process, which further suggests that the XRD peak detected by the
453 *CheMin* instrument onboard *Curiosity* at 9.22 Å is very unlikely explained by the presence of such a
454 mineral phase. The detailed XRD data have not been released to the public yet, so we did not have
455 access to that data. We based our discussion on the preliminary interpretations given by the
456 MSL/CheMin team at the Lunar and Planetary Science Conference earlier this year. We will need to wait
457 for further analyses and communications by this team to identify the nature of the 9.22 Å peak that was
458 initially reported as being potentially Jahnsite.

459

460 **Acknowledgements**

461 We acknowledge the support from the Agence Nationale de la recherche (ANR) under the contract ANR-
462 16-CE31-0012 entitled Mars-Prime. We would also like to thank David Kinniburgh for helpful discussions
463 about PHREEPLOT. Finally, we thank Allan Treiman (plus an anonymous reviewer) for reviewing this work.

464

465

References

Abboud, I.A. (2008). Mineralogy and chemistry of urinary stones: patients from North Jordan. *Environmental geochemistry and health* **30 (5)**:445-463. doi: 10.1007/s10653-007-9128-7.

Alhakmi, G., Assani, A., Saadi, M., and El Ammari, L. (2018). Synthesis and crystal structure of two new phosphates with Alluaudite type structure: (M, Mn)3Fe(PO4)3 (M= Ca, Cd). *MATEC Web Conf.* 149.

Appelo, C. A. J., Parkhurst, D. L., and Post, V. E. A. (2014). Equations for calculating hydrogeochemical reactions of minerals and gases such as CO2 at high pressures and temperatures. *Geochimica et Cosmochimica Acta* **125**:49-67. doi: https://doi.org/10.1016/j.gca.2013.10.003.

Baijot, M, Hatert F., Dal Bo, F., and Philippo, S. (2014). Mineralogy and petrography of phosphate mineral associations from the Jocao pegmatite, Minas Gerais, BRazil. *The Canadian Mineralogist* **52 (2)**:373-397. doi: 10.3749/canmin.52.2.373.

Barin, I. (1993a). Ag-AuTe2. In *Thermochemical Data of Pure Substances*, 2nd edition, VCH, Weinheim, ISBN: 3-527-28531-8, 1-103.

Barin, I. (1993b). D-FeWO4. In *Thermochemical Data of Pure Substances*, 2nd edition, VCH, Weinheim, ISBN: 3-527-28531-8, 635-727.

Blanc, P., Lassin, A., Piantone, P., Azaroual, M., Jacquemet, N., Fabbri, A., and Gaucher, E.C. (2012). Thermoddem: A geochemical database focused on low temperature water/rock interactions and waste materials. *Applied Geochemistry* **27 (10)**:2107-2116. doi: https://doi.org/10.1016/j.apgeochem.2012.06.002.

Bridges, J.C., Schwenzer, S.P., Leveille, R., Westall, F., Wiens, R.C., Mangold, N., Bristow, T., Edwards, P., and Berger, G. (2015). Diagenesis and clay mineral formation at Gale Crater, Mars. *Journal of Geophysical Research: Planets* **120 (1)**:1-19. doi: https://doi.org/10.1002/2014JE004757.

Capitelli, F., Chita, G., Cavallo, A., Bellatreccia, F., and Della Ventura, G. (2011). Crystal structure of whiteite-(CaFeMg) from Crosscut Creek, Canada. **226 (9)**:731-738. doi: doi:10.1524/zkri.2011.1393.

Cassedanne, J.P., and Baptista, A. (1999). Famous Mineral Localities: The Sapucaia Pegmatite Minas Gerais, Brazil. *Mineralogical Record* **30**:347-360.

Di Cossato, Y., Fecia, M., Orlandi, P., and Vezzalini, G. (1989). Rittmannite, a new mineral species of the whiteite group from the Mangualde granitic pegmatite, Portugal. *The Canadian Mineralogist* **27 (3)**:447-449.

Drouet, C, and Navrotsky, A. (2003). Synthesis, characterization, and thermochemistry of K-Na-H3O jarosites. *Geochimica et Cosmochimica Acta* **67 (11)**:2063-2076. doi: 10.1016/S0016-7037(02)01299-1.

Drouet, C. (2015). A comprehensive guide to experimental and predicted thermodynamic properties of phosphate apatite minerals in view of applicative purposes. *The Journal of Chemical Thermodynamics* **81**:143-159. doi: http://dx.doi.org/10.1016/j.jct.2014.09.012.

Drouet, C. (2019). Applied predictive thermodynamics (ThermAP). Part 2. Apatites containing Ni2+, Co2+, Mn2+, or Fe2+ ions. *The Journal of Chemical Thermodynamics* **136**:182-189. doi: https://doi.org/10.1016/j.jct.2015.06.016.

Drouet, C., and Alphonse, P. (2015). ThermAP additive model for applied predictive thermodynamics. In *Therm'AP free calculation program,* www.christophedrouet.com/thermAP.html (accessed date: Sept. 2021), Toulouse, France.

Elliott, P. (2016). Jahnsite-(CaFeMg), a new mineral from Tom's quarry, South Australia: description and crystal structure. *European Journal of Mineralogy* **28 (5)**:991-996. doi: 10.1127/ejm/2016/0028-2562.

Elliott, P., and Willis, A.C. (2019). Whiteite-(mnmnmg), a New Jahnsite-Group Mineral from Iron Monarch, South Australia: Description and Crystal Structure. *The Canadian Mineralogist* **57 (2)**:215-223. doi: 10.3749/canmin.1800070.

Grey, I. E., Mumme, W.G., Neville, S.M., Wilson, N.C., and Birch, W.D. (2010). Jahnsite—whiteite solid solutions and associated minerals in the phosphate pegmatite at Hagendorf-Süd, Bavaria, Germany. *Mineralogical Magazine* **74 (6)**:969-978. doi: 10.1180/minmag.2010.074.6.969.

Grey, I.E., Keck, E., Kampf, A.R., MacRae, C.M., Cashion, J.D., and Glenn, A.M. (2020). Jahnsite-(CaMnZn) from the Hagendorf-Süd pegmatite, Oberpfalz, Bavaria, and structural flexibility of jahnsite-group minerals. *Mineralogical Magazine* **84 (4)**:547-553. doi: 10.1180/mgm.2020.40.

Grice, J.D., Dunn, P.J., and Ramik, R.A. (1989). Whiteite-(CaMnMg), a new species from the Tip Top Pegmatite, Custer, South Dakota. *The Canadian Mineralogist* **27 (4)**:699-702.

Grice, J.D., Dunn, P.J., and Ramik, R.A. (1990). Jahnsite-(CaMnMn), a new member of the whiteite group from Mangualde, Beira, Portugal. *American Mineralogist* **75 (3-4)**:401-404.

Helgeson, H.C. (1978). *Summary and critique of the thermodynamic properties of rock-forming minerals*. New Haven: Kline Geology Laboratory, Yale University.

Kampf, A.R., Adams, P.M., and Nash, B.P. (2016). Whiteite-(camgmg), CaMg3Al2(PO4)4(OH)2·8H2O, a New Jahnsite-group Mineral from the Northern Belle Mine, Candelaria, Nevada, U.S.A. *The Canadian Mineralogist* **54 (6)**:1513-1523. doi: 10.3749/canmin.1600051.

Kampf, A.R., Alves, P., Kasatkin, A., and Škoda, R. (2019). Jahnsite-(MnMnZn), a new jahnsite-group mineral, and formal approval of the jahnsite group. *European Journal of Mineralogy* **31 (1)**:167-172. doi: 10.1127/ejm/2018/0030-2800.

Kampf, A.R., Elliott, P., Nash, B.P., Chiappino, L., and Varvello, S. (2018). Jahnsite-(NaMnMg), A New Jahnsite-Group Mineral from the Sapucaia Mine, Brazil and the White Rock No. 2 Quarry, Australia. *The Canadian Mineralogist* **56 (6)**:871-882. doi: 10.3749/canmin.1800053.

Kampf, A.R., Steele, I.M., and Loomis, T.A. (2008). Jahnsite-(NaFeMg), a new mineral from the Tip Top mine, Custer County, South Dakota: Description and crystal structure. *American Mineralogist* **93 (5-6)**:940-945. doi: doi:10.2138/am.2008.2771.

Kinniburgh, D., and Cooper, D. (2011). *PhreePlot: Creating graphical output with PHREEQC*. In *Software user manual*.

Kurokawa, H., Kurosawa, K., and Usui, T. (2018). A lower limit of atmospheric pressure on early Mars inferred from nitrogen and argon isotopic compositions. *Icarus* **299**:443-459. doi: https://doi.org/10.1016/j.icarus.2017.08.020.

La Iglesia, A. (2009). Estimating the thermodynamic properties of phosphate minerals at high and low temperature from the sum of constituent units. *Estudios Geologicos-Madrid* **65 (2)**:109-119. doi: 10.3989/egeol.39849.060.

Lanza, N., Gasda, P., Essunfeld, A., Comellas, J., Caravaca, G., Rampe, E., Williams, A., Meslin, P.Y., Dehouck, E., Mangold, N., Rapin, W., Hazen, R., Fischer, W., Ollila, A., House, C., and Wiens, R. (2021). Chemistry of Manganese-Bearing Materials at the Groken Drill Site, Gale Crater, Mars. 52nd Lunar and Planetary Science Conference, 2021/03/15-19.

McConnochie, T.H., Smith, M.D., Wolff, M.J., Bender, S., Lemmon, M., Wiens, R.C., Maurice, S., Gasnault, O., Lasue, J., Meslin, P.Y., Harri, A.M., Genzer, M., Kemppinen, O., Martínez, G.M., DeFlores, L., Blaney, D., Johnson, J.R., and Bell, J.F. (2018). Retrieval of water vapor column abundance and aerosol properties from ChemCam passive sky spectroscopy. *Icarus* **307**:294-326. doi: https://doi.org/10.1016/j.icarus.2017.10.043.

Miyawaki, R., Hatert, F., Pasero, M., and Mills, S.J. (2019). New minerals and nomenclature modifications approved in 2019. *Mineralogical Magazine* **83 (6)**:887-893. doi: 10.1180/mgm.2019.73.

Moore, P.B., and Araki, T. (1974). *Jahnsite, CaMnMg2(H2O)8Fe2(OH)2[PO4]4: A novel stereoisomerism of ligands about octahedral corner-chains*. *American Mineralogist* **59**:964-973.

Moore, P., and Itô, J. (1974). I. Jahnsite, Segelerite, and Robertsite, Three New Transition Metal Phosphate Species II. Redefinition of Overite, an Isotype of Segelerite III. Isotypy of Robertsite, Mitridatite, and Arseniosiderite. *American Mineralogist* **59**:48-59.

Mücke, A. (1979). Keckite, (CaMg)(Mn,Zn)2Fe3+2[(OH)2(PO4)4]·2H2O, ein neues Mneral von agendrof/Obf. und seine genetische Stellung. *Neues Jahrbuch für Mineralogie, Abhandlungen* **134**:183-192.

Navrotsky, A., Forray, F.L., and Drouet, C. (2005). Jarosite stability on Mars. *Icarus* **176**:250-253. doi: 10.1016/j.icarus.2005.02.003.

Parkhurst, D.L., and Appelo, C.A.J. (2013). Description of input and examples for PHREEQC version 3—A computer program for speciation, batch-reaction, one-dimensional transport, and inverse geochemical calculations. In *U.S. Geological Survey Techniques and Methods*, 497 p.

Trainer, M.G., Wong, M.H., McConnochie, T.H., Franz, H.B., Atreya, S.K., Conrad, P.G., Lefèvre, F., Mahaffy, P.R., Malespin, C.A., Manning, H.L.K., Martín-Torres, J., Martínez, G.M., McKay, C.P., Navarro-González, R., Vicente-Retortillo, A., Webster, C.R., and Zorzano, M.P. (2019). Seasonal Variations in Atmospheric Composition as Measured in Gale Crater, Mars. *Journal of Geophysical Research: Planets* **124 (11)**:3000-3024. doi: https://doi.org/10.1029/2019JE006175.

Treiman, A.H., Downs, R.T., Ming, D.W., Morris, R.V., Thorpe, M.T., Hazen, R.M., Downs, G.W., Rampe, E.B., and the *CheMin* Team (2021). Possible Detection of a Jahnsite-Whiteite Group Phosphate Mineral by MSL CheMin in Glen Torridon, Gale Crater, Mars. 52nd Lunar and Planetary Science Conference, 2021/03/1.

Vasavada, A.R., Piqueux, S., Lewis, K.W., Lemmon, M.T., and Smith, M.D. (2017). Thermophysical properties along Curiosity's traverse in Gale crater, Mars, derived from the REMS ground temperature sensor. *Icarus* **284**:372-386. doi: https://doi.org/10.1016/j.icarus.2016.11.035.

583 Vieillard, P., and Tardy, Y. (1984). Thermochemical Properties of Phosphates. In *Phosphate Minerals*,
584 edited by JeromeO Nriagu and PaulB Moore, 171-198. Springer Berlin Heidelberg.
585 Vignola, P., Hatert, F., Baijot, M., Rotiroti, N., Risplendente, A., and Varvello, S. (2019). Jahnsite-
586 (MnMnMg), Mn2+Mn2+Mg2+2Fe3+2(PO4)4(OH)2·8H2O, a New Phosphate Mineral Species from
587 Sapucaia Pegmatite, Sapucaia Do Norte, Galiléia, Minas Gerais, Brazil. *The Canadian*
588 *Mineralogist* **57 (3)**:363-370. doi: 10.3749/canmin.1800078.

589

590

591

This is the peer-reviewed, final accepted version for American Mineralogist, published by the Mineralogical Society of America.
The published version is subject to change. Cite as Authors (Year) Title. American Mineralogist, in press.
DOI: https://doi.org/10.2138/am-2022-8174. http://www.minsocam.org/

Table captions

Table 1. Overview of the main Jahnsite and Whiteite end-member compositions established to-date: reference names, chemical compositions, illustrative localities on Earth and related references.

Table 2. Values g_i , h_i and s_i as determined by the *ThermAP* predictive model, for the estimation of $\Delta G_f°$, $\Delta H_f°$ or S° of Jahnsites/Whiteites (at T = 298 K, 1 bar) from their ionic composition.

Table 3. Recommended thermodynamic properties for several Jahnsite/Whiteite end-members based on *ThermAP* refinements.

Figure captions

Figure 1. Jahnsite/Whiteite structure of phases viewed along the direction [010]. The dashed line refers to one unit cell. The a and b lettering for M2 and M3 sites denote two existing orientations. Used by permission of Mineralogical Association of Canada, from Kampf et al. (2018), The Canadian Mineralogist, vol. 56 (6), Fig. 5, p. 881.

Figure 2. Comparison of $\Delta G_f°$ values as calculated via *ThermAP* (using the g_i values tabulated on **Table 2**) with reference data (Thermoddem database).

Figure 3. Comparison of S° values as calculated via *ThermAP* (using the s_i values tabulated in **Table 2**) with reference data (Thermoddem database).

Figure 4. Comparison of $\Delta H_f°$ values as calculated via *ThermAP* (relating to the h_i values tabulated on **Table 2**) with available reference data (Thermoddem database). The notation "n.d." stands for "not determined" due to unknown reference enthalpy data for these compounds.

Figure 5. (**a**) Saturation index (pH not fixed) without allowing precipitation, in equilibrium with or isolated from the terrestrial atmosphere (to potentially mimic laboratory experiments). (**b**) Precipitation of predominant phases (same conditions but enabling phase precipitation). The notation "cor" refers to the phases that have been "corrected" compared to the Thermoddem database (see text).

Figure 6. Predominance diagrams in the log $f(O_2)$-pH space (PHREEPLOT), starting from similar concentration and elemental ratios to Figure 5 (Fe 0.6 / Mg 0.6 / Mn 0.3 / Ca 0.3 / P 1.2 mol/kg), and considering a terrestrial pCO_2 of 400 ppm.

Figure 7. XRD pattern for the experimentally precipitated compound, starting from the initial stoichiometry of Jahnsite-(CaMnMg), at 100°C for 24 hours. Letters "S" and "P" refer to the $FePO_4 : 2H_2O$ polymorphs Strengite and Phosphosiderite, respectively.

Figure 8. Evaluation of the stability fields of Jahnsites-(CaMnMn), (CaMnMg) and (MnMnMg) and corresponding Alluaudites in the $f(H_2O)$-T space. The dotted grey lines represent, for information, the H_2O phase diagram. The yellow dotted box shows the typical min and max temperature and $f(H_2O)$ values measured by Curiosity at Gale Crater (McConnochie et al. 2018).

This is the peer-reviewed, final accepted version for American Mineralogist, published by the Mineralogical Society of America.
The published version is subject to change. Cite as Authors (Year) Title. American Mineralogist, in press.
DOI: https://doi.org/10.2138/am-2022-8174. http://www.minsocam.org/

681 **Tables**

Sample	Composition	Origin (locality)	Ref.
	Jahnsites		
Jahnsite-(CaMnMg)	$CaMnMg_2Fe_2(PO_4)_4(OH)_2 : 8H_2O$	Custer County, South Dakota, USA	(Moore and Araki 1974)
Jahnsite-(CaMnMn)	$CaMnMn_2Fe_2(PO_4)_4(OH)_2 : 8H_2O$	Mangualde, Portugal	(Grice, Dunn, and Ramik 1990)
Jahnsite-(CaFeMg)	$CaFeMg_2Fe_2(PO_4)_4(OH)_2 : 8H_2O$	Mt Lofty Ranges, Australia	(Elliott 2016)
Jahnsite-(MnMnMg)	$MnMnMg_2Fe_2(PO_4)_4(OH)_2 : 8H_2O$	Minas Gerais, Brazil	(Vignola et al. 2019)
Jahnsite-(NaMnMg)	*	Minas Gerais, Brazil; Quarry, Australia	(Kampf et al. 2018)
Jahnsite-(NaMnMn)	**	Quarry, Australia	(Miyawaki et al. 2019)
Jahnsite-(CaMnFe)	$CaMnFe_2Fe_2(PO_4)_4(OH)_2 : 8H_2O$	Minas Gerais, Brazil	(Cassedanne and Baptista 1999)
Jahnsite-(MnMnMn)	$MnMnMn_2Fe_2(PO_4)_4(OH)_2 : 8H_2O$	Minas Gerais, Brazil	(Baijot et al. 2014)
Jahnsite-(MnMnZn)	$MnMnZn_2Fe_2(PO_4)_4(OH)_2 : 8H_2O$	Herdade dos Pendoes, Portugal	(Kampf et al. 2019)
Jahnsite-($NaFe^{III}Mg$)	$NaFe^{III}Mg_2Fe_2(PO_4)_4(OH)_2 : 8H_2O$	Custer County, South Dakota, USA	(Kampf, Steele, and Loomis 2008)
Jahnsite-(CaMnZn)	$CaMnZn_2Fe_2(PO_4)_4(OH)_2 : 8H_2O$	Hagendorf-Süd, Bavaria, Germany	(Grey et al. 2020)
Jahnsite-(CaMnMn/Fe) aka *Keckite*	$CaMn(Mn/Fe)_2Fe_2(PO_4)_4(OH)_2 : 8H_2O$	Hagendorf-Süd, Bavaria, Germany	(Kampf, Steele, and Loomis 2008; Mücke 1979)
	Whiteites		
Whiteite-(CaMnMn)	$CaMnMn_2Al_2(PO_4)_4(OH)_2 : 8H_2O$	Hagendorf-Süd, Bavaria, Germany	(Grey et al. 2010)
Whiteite-(MnMnMg)	$MnMnMg_2Al_2(PO_4)_4(OH)_2 : 8H_2O$	Iron Monarch, Australia	(Elliott and Willis 2019)
Whiteite-(MnMnFe) aka *Rittmannite*	$MnMnFe_2Al_2(PO_4)_4(OH)_2 : 8H_2O$	Mangualde, Portugal	(di Cossato, Orlandi, and Vezzalini 1989)
Whiteite-(CaFeMg)	$CaFeMg_2Al_2(PO_4)_4(OH)_2 : 8H_2O$	Crosscut Creek, Canada	(Capitelli et al. 2011)
Whiteite-(CaMnMg)	$CaMnMg_2Al_2(PO_4)_4(OH)_2 : 8H_2O$	Custer County, South Dakota, USA	(Grice, Dunn, and Ramik 1989)
Whiteite-(CaMgMg)	$CaMgMg_2Al_2(PO_4)_4(OH)_2 : 8H_2O$	Candelaria, Nevada, U.S.A.	(Kampf, Adams, and Nash 2016)

682 *The authors named this compound in link with ions predominant occupation in the X, M1, M2 and M3 sites; however
683 additional ions occurred in the chemical formula to allow electroneutrality. For instance, the following formula was given for the
684 Brazilian sample $(Na_{0.56}Ca_{0.25}Mn_{0.09})(Mn_{0.85}Fe^{III}_{0.15})(Mg_{1.53}Fe^{III}_{0.47})(Fe^{III}_{1.79}Al_{0.21})(PO_4)_4(OH)_{1.83}: H_2O_{8.17}$.
685 **Similarly, for this compound, additional ions occur in the structure to maintain the electroneutrality such Fe^{3+} in M2 sites,
686 giving the overall formula $NaMn(MnFe^{III})Fe^{III}_2(PO_4)_4(OH)_2 : 8H_2O$.
687

688 **Table 1.** Overview of the main Jahnsite and Whiteite end-member compositions established to-date: reference names, chemical
689 compositions, illustrative localities on Earth and related references.

This is the peer-reviewed, final accepted version for American Mineralogist, published by the Mineralogical Society of America.
The published version is subject to change. Cite as Authors (Year) Title. American Mineralogist, in press.
DOI: https://doi.org/10.2138/am-2022-8174. http://www.minsocam.org/

Contributing ions at 298 K, 1 bar	g_i (kJ/mol)	h_i (kJ/mol)	s_i ($J.mol^{-1}.K^{-1}$)
Cations			
Ca^{2+}	-747.1	-776.4	47.2
Mg^{2+}	-638.0	-669.3	30.2
Mn^{2+}	-443.0	-462.1	70.5
Fe^{2+}	-279.0	-290.8	90.2
Zn^{2+}	-350.7	-367.1	70.0
Fe^{3+}	-353.1	-391.5	52.0
Al^{3+}	-796.2	-845.9	15.3
Na^{+}	-334.6	-353.6	39.1
K^{+}	-375.5	-398.0	40.6
H^{+}	-110.4	-137.7	25.1
Anions			
PO_4^{3-}	-821.7	-897.3	44.0
OH^{-}	-115.8	-140.6	33.4
F^{-}	-278.1	-287.1	19.9
Hydration			
H_2O	-237.1	-295.4	37.6

Table 2. Values g_i , h_i and s_i as determined by the *ThermAP* predictive model, for the estimation of $\Delta G_f°$, $\Delta H_f°$ or S° of Jahnsites/Whiteites (at T = 298 K, 1 bar) from their ionic composition.

This is the peer-reviewed, final accepted version for American Mineralogist, published by the Mineralogical Society of America.
The published version is subject to change. Cite as Authors (Year) Title. American Mineralogist, in press.
DOI: https://doi.org/10.2138/am-2022-8174. http://www.minsocam.org/

Compound at 298 K, 1 bar	$\Delta G_f°$ (kJ/mol)	$\Delta H_f°$ (kJ/mol)	$S°$ (J.mol^{-1}.K^{-1})	log K *
Jahnsites				
Jahnsite-(CaMnMg)	-8588	-9594	826	10.4
Jahnsite-(CaMnMn)	-8198	-9179	906	-0.1
Jahnsite-(CaFeMg)	-8424	-9422	845	14.6
Jahnsite-(MnMnMg)	-8283	-9279	849	7.2
Jahnsite-(CaMnFe)	-7870	-8837	946	8.3
Jahnsite-(MnMnMn)	-7893	-8865	930	-3.3
Jahnsite-(MnMnZn)	-7709	-8675	929	-0.1
Jahnsite-(NaFe^{III}Mg)	-8085	-9100	799	9.9
Jahnsite-(CaMnZn)	-8013	-8989	905	3.1
Whiteites				
Whiteite-(CaMnMn)	-9084	-10088	833	9.8
Whiteite-(MnMnMg)	-9170	-10188	776	17.1
Whiteite-(MnMnFe) aka *Rittmannite*	-8452	-9431	896	15.1
Whiteite-(CaFeMg)	-9310	-10331	772	24.5
Whiteite-(CaMnMg)	-9474	-10502	752	20.3
Whiteite-(CaMgMg)	-9669	-10710	712	25.5

**log K values refer to the dissolution of the phase considering the $H_2PO_4^-$ phosphate speciation.*

Table 3. Recommended thermodynamic properties for several Jahnsite/Whiteite end-members based on *ThermAP* refinements.

This is the peer-reviewed, final accepted version for American Mineralogist, published by the Mineralogical Society of America.
The published version is subject to change. Cite as Authors (Year) Title. American Mineralogist, in press.
DOI: https://doi.org/10.2138/am-2022-8174. http://www.minsocam.org/

Figures

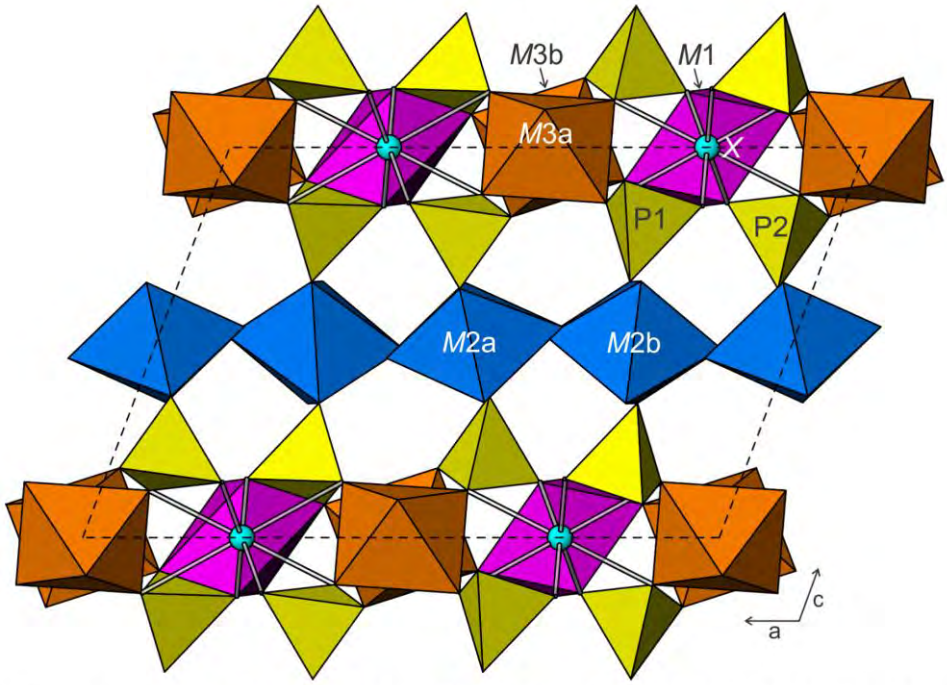

Figure 1. Jahnsite/Whiteite structure of phases viewed along the direction [010]. The dashed line refers to one unit cell. The a and b lettering for M2 and M3 sites denote two existing orientations. Used by permission of Mineralogical Association of Canada, from Kampf et al. (2018), The Canadian Mineralogist, vol. 56 (6), Fig. 5, p. 881.

This is the peer-reviewed, final accepted version for American Mineralogist, published by the Mineralogical Society of America.
The published version is subject to change. Cite as Authors (Year) Title. American Mineralogist, in press.
DOI: https://doi.org/10.2138/am-2022-8174. http://www.minsocam.org/

718

719 **Figure 2.** Comparison of $\Delta G_f°$ values as calculated via *ThermAP* (using the g_i values tabulated on **Table 2**) with reference data

720 (Thermoddem database).

721

This is the peer-reviewed, final accepted version for American Mineralogist, published by the Mineralogical Society of America.
The published version is subject to change. Cite as Authors (Year) Title. American Mineralogist, in press.
DOI: https://doi.org/10.2138/am-2022-8174. http://www.minsocam.org/

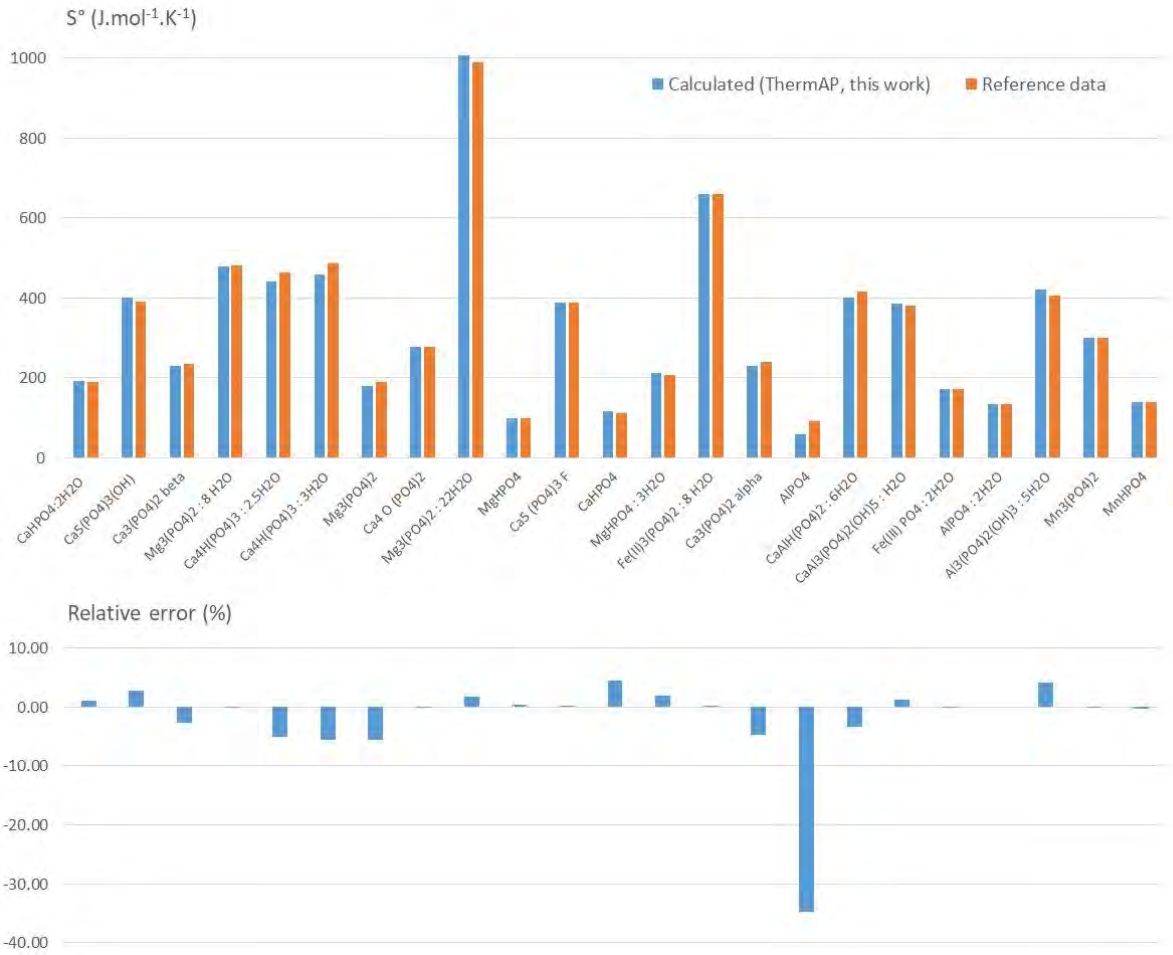

Figure 3. Comparison of S° values as calculated via *ThermAP* (using the s_i values tabulated in **Table 2**) with reference data (Thermoddem database).

This is the peer-reviewed, final accepted version for American Mineralogist, published by the Mineralogical Society of America.
The published version is subject to change. Cite as Authors (Year) Title. American Mineralogist, in press.
DOI: https://doi.org/10.2138/am-2022-8174. http://www.minsocam.org/

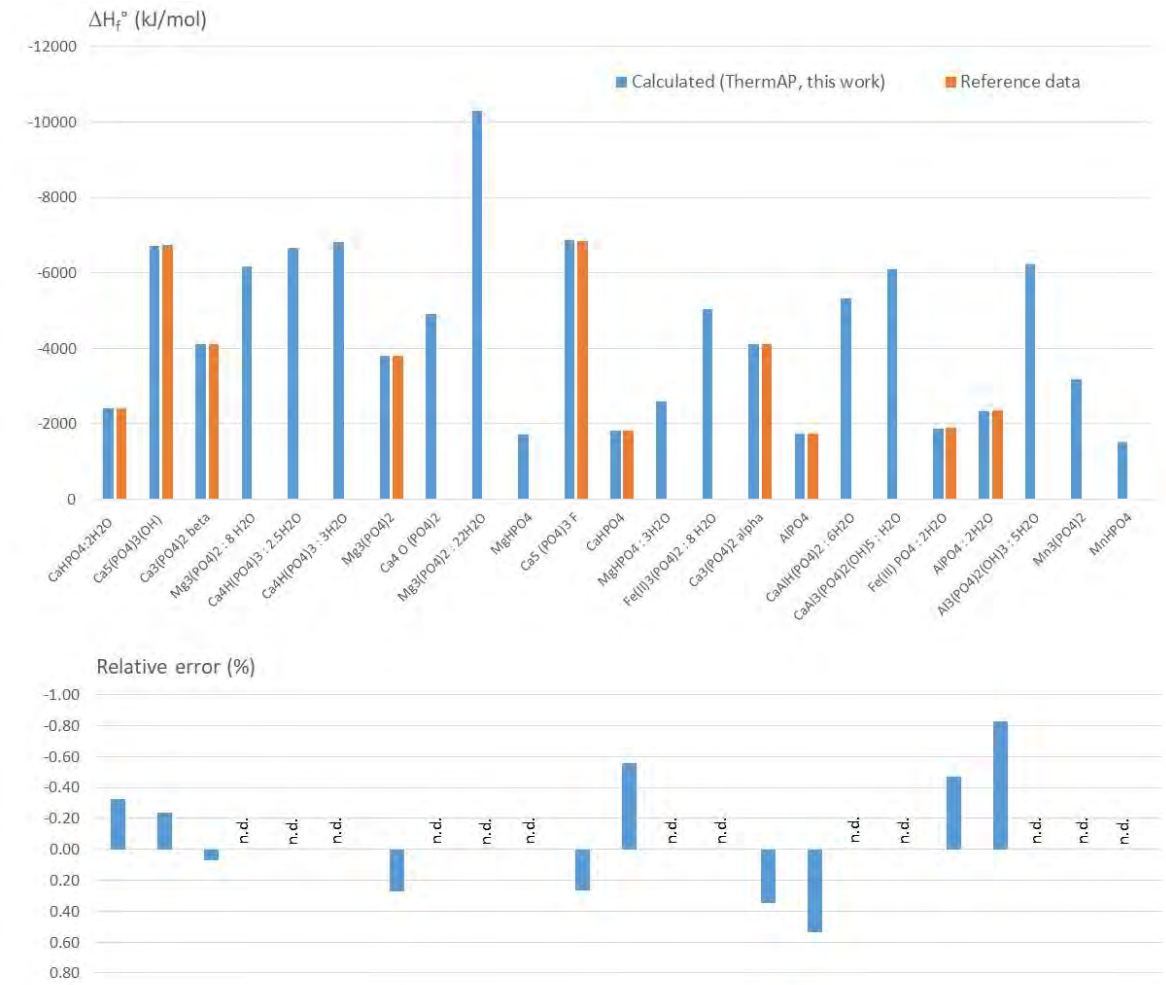

727

728 **Figure 4.** Comparison of $\Delta H_f°$ values as calculated via *ThermAP* (relating to the h_i values tabulated on **Table 2**) with available
729 reference data (Thermoddem database). The notation "n.d." stands for "not determined" due to unknown reference enthalpy
730 data for these compounds.

731

732

This is the peer-reviewed, final accepted version for American Mineralogist, published by the Mineralogical Society of America.
The published version is subject to change. Cite as Authors (Year) Title. American Mineralogist, in press.
DOI: https://doi.org/10.2138/am-2022-8174. http://www.minsocam.org/

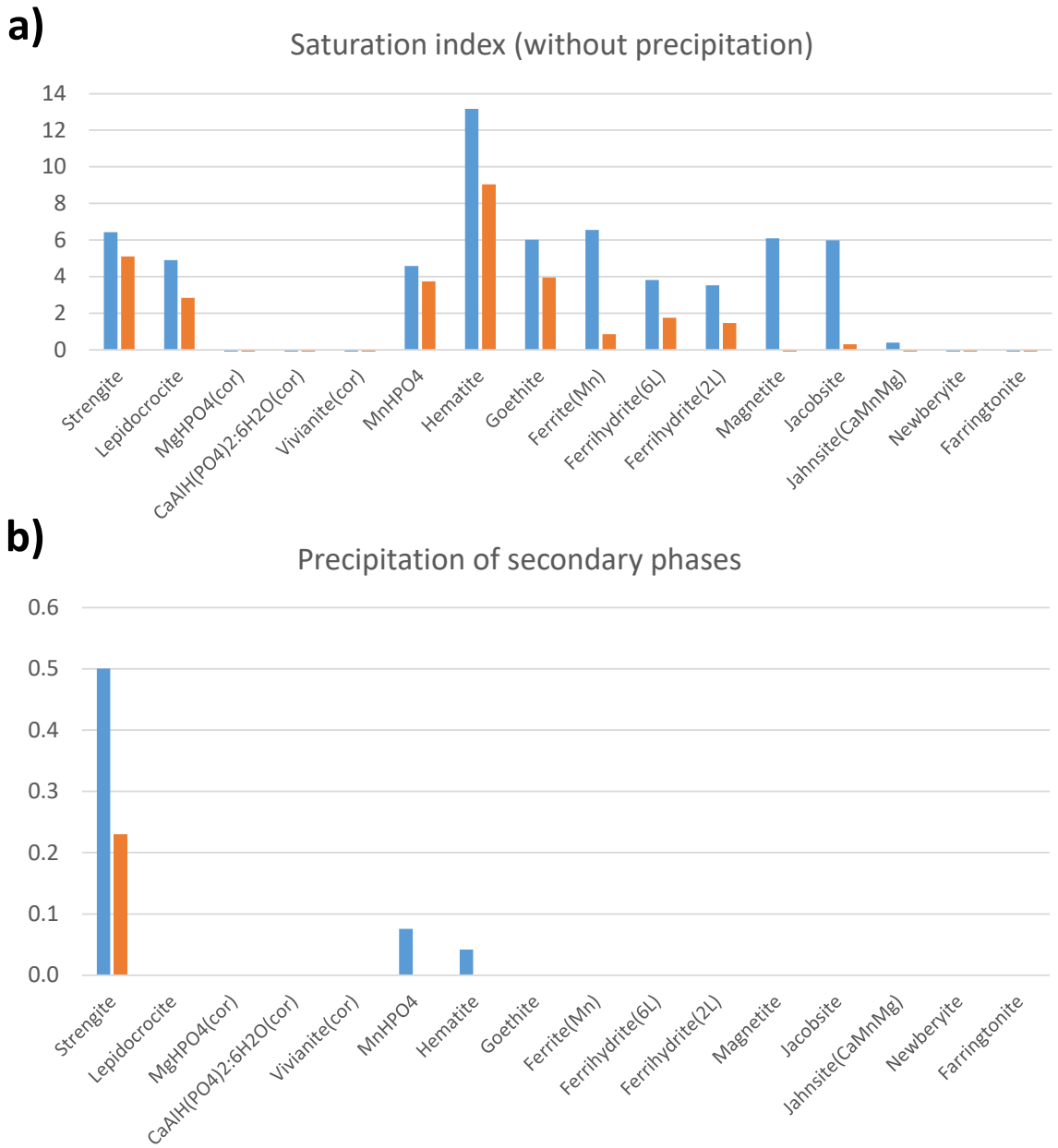

Figure 5. (**a**) Saturation index (pH not fixed) without allowing precipitation, in equilibrium with or isolated from the terrestrial atmosphere (to potentially mimic laboratory experiments). (**b**) Precipitation of predominant phases (same conditions but enabling phase precipitation). The notation "cor" refers to the phases that have been "corrected" compared to the Thermoddem database (see text).

This is the peer-reviewed, final accepted version for American Mineralogist, published by the Mineralogical Society of America.
The published version is subject to change. Cite as Authors (Year) Title. American Mineralogist, in press.
DOI: https://doi.org/10.2138/am-2022-8174. http://www.minsocam.org/

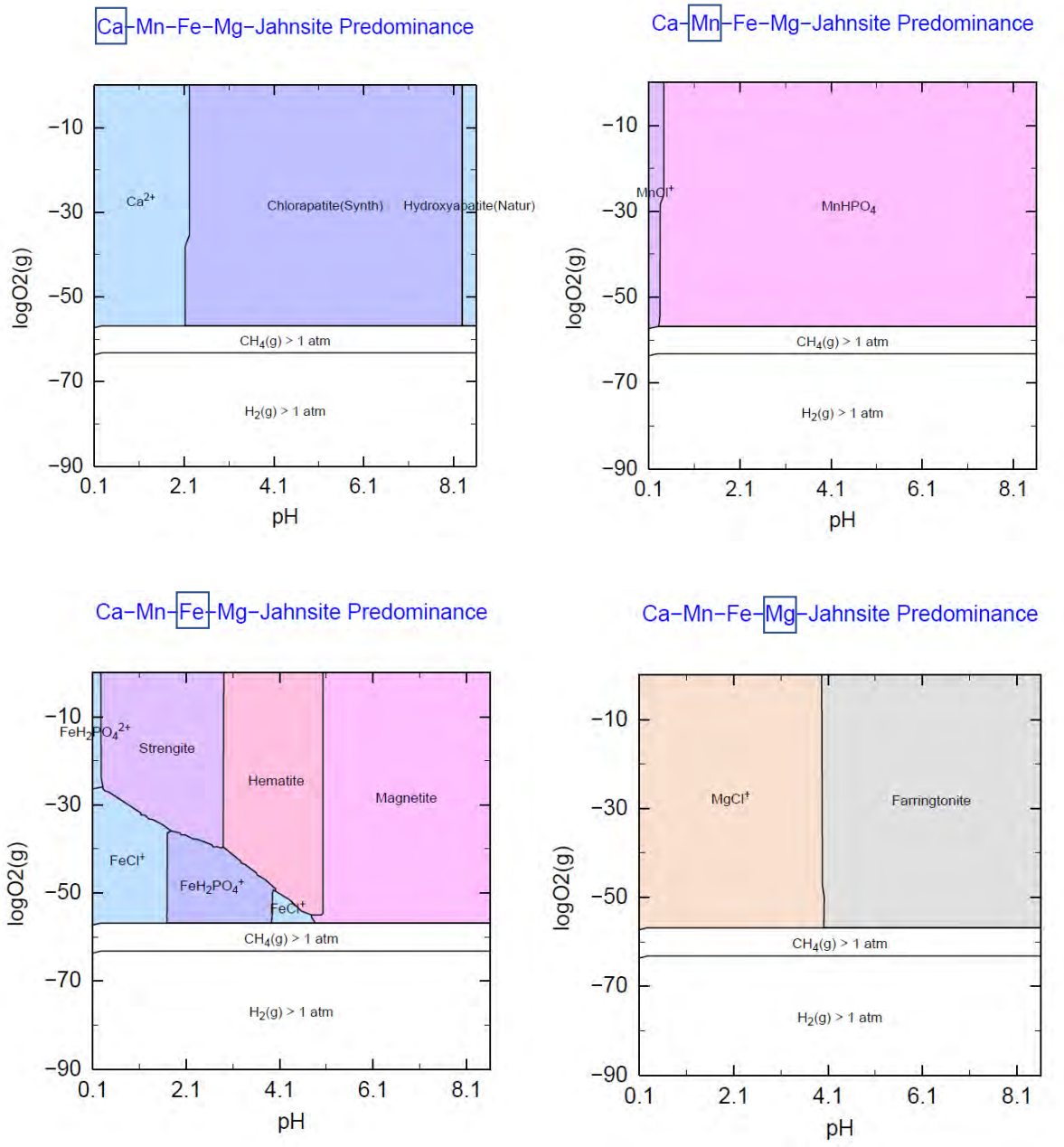

Figure 1 – Calcul de prédominance logO2 – pH sur PHREEPLOT, en partant d'une même concentration et d'un même ratio entre éléments qu'avec les sels. (Fe : 0.6 / Mg : 0.6 /Mn : 0.3 / Ca : 0.3 /P : 1.2 moles /kg)

Figure 6. Predominance diagrams in the log $f(O_2)$-pH space (PHREEPLOT), starting from similar concentration and elemental ratios to Figure 5 (Fe 0.6 / Mg 0.6 / Mn 0.3 / Ca 0.3 / P 1.2 mol/kg), and considering a terrestrial pCO_2 of 400 ppm.

This is the peer-reviewed, final accepted version for American Mineralogist, published by the Mineralogical Society of America.
The published version is subject to change. Cite as Authors (Year) Title. American Mineralogist, in press.
DOI: https://doi.org/10.2138/am-2022-8174. http://www.minsocam.org/

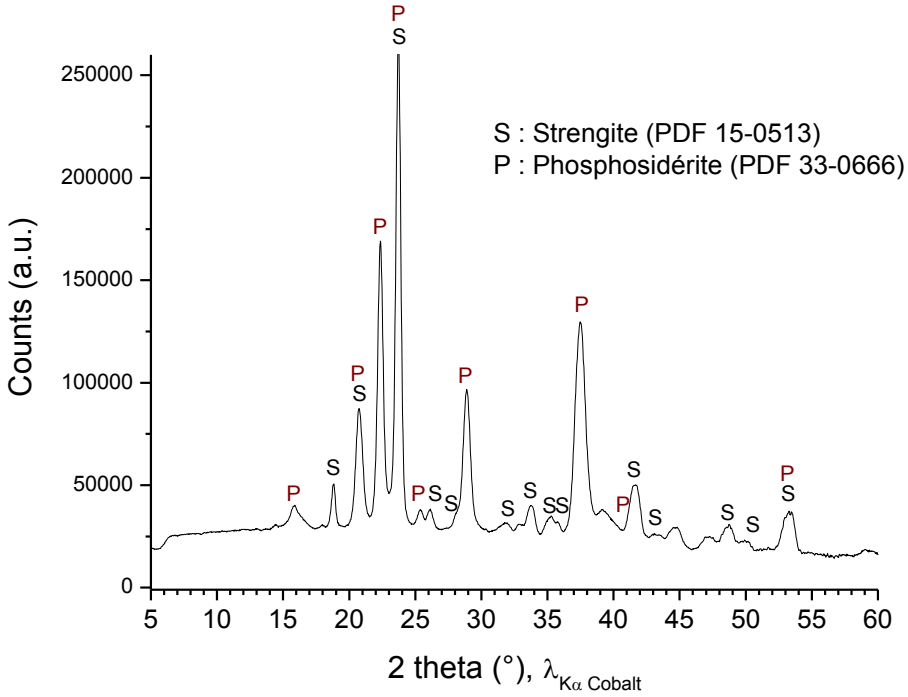

744

745 **Figure 7.** XRD pattern for the experimentally precipitated compound, starting from the initial stoichiometry of Jahnsite-
746 (CaMnMg), at 100°C for 24 hours. Letters "S" and "P" refer to the $FePO_4 : 2H_2O$ polymorphs Strengite and Phosphosiderite,
747 respectively.

748

749

750

This is the peer-reviewed, final accepted version for American Mineralogist, published by the Mineralogical Society of America.
The published version is subject to change. Cite as Authors (Year) Title. American Mineralogist, in press.
DOI: https://doi.org/10.2138/am-2022-8174. http://www.minsocam.org/

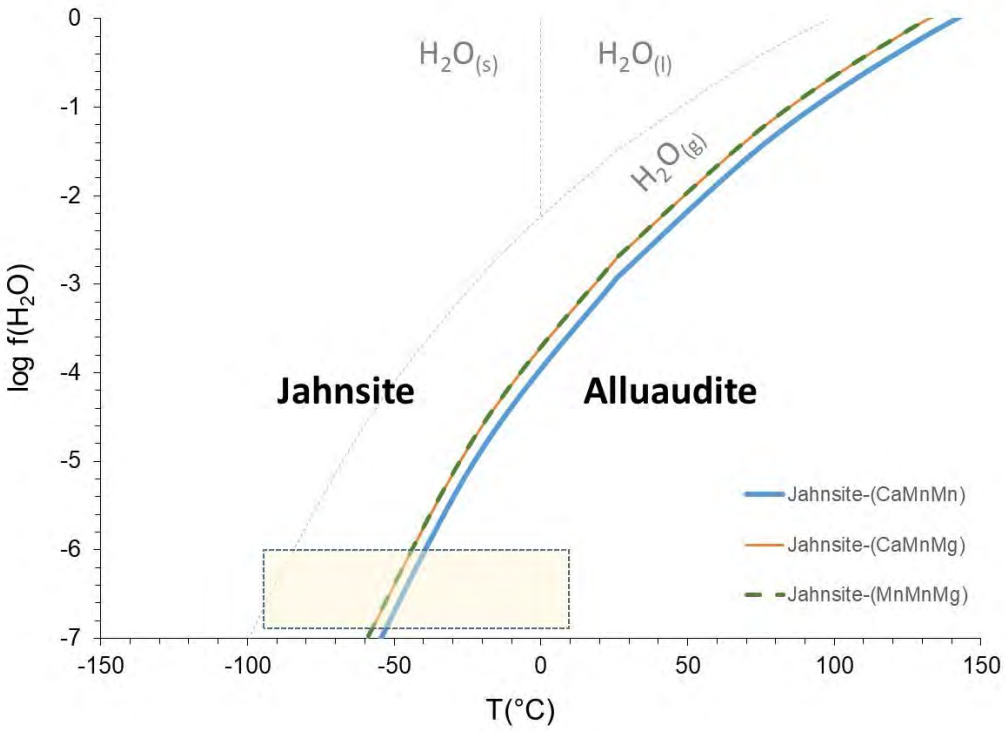

751

752 **Figure 8.** Evaluation of the stability fields of Jahnsites-(CaMnMn), (CaMnMg) and (MnMnMg) and corresponding Alluaudites in
753 the $f(H_2O)$-T space. The dotted grey lines represent, for information, the H_2O phase diagram. The yellow dotted box shows the
754 typical min and max temperature and $f(H_2O)$ values measured by Curiosity at Gale Crater (McConnochie et al. 2018).

755

756

757

758

759

760

761

762

Figure 1

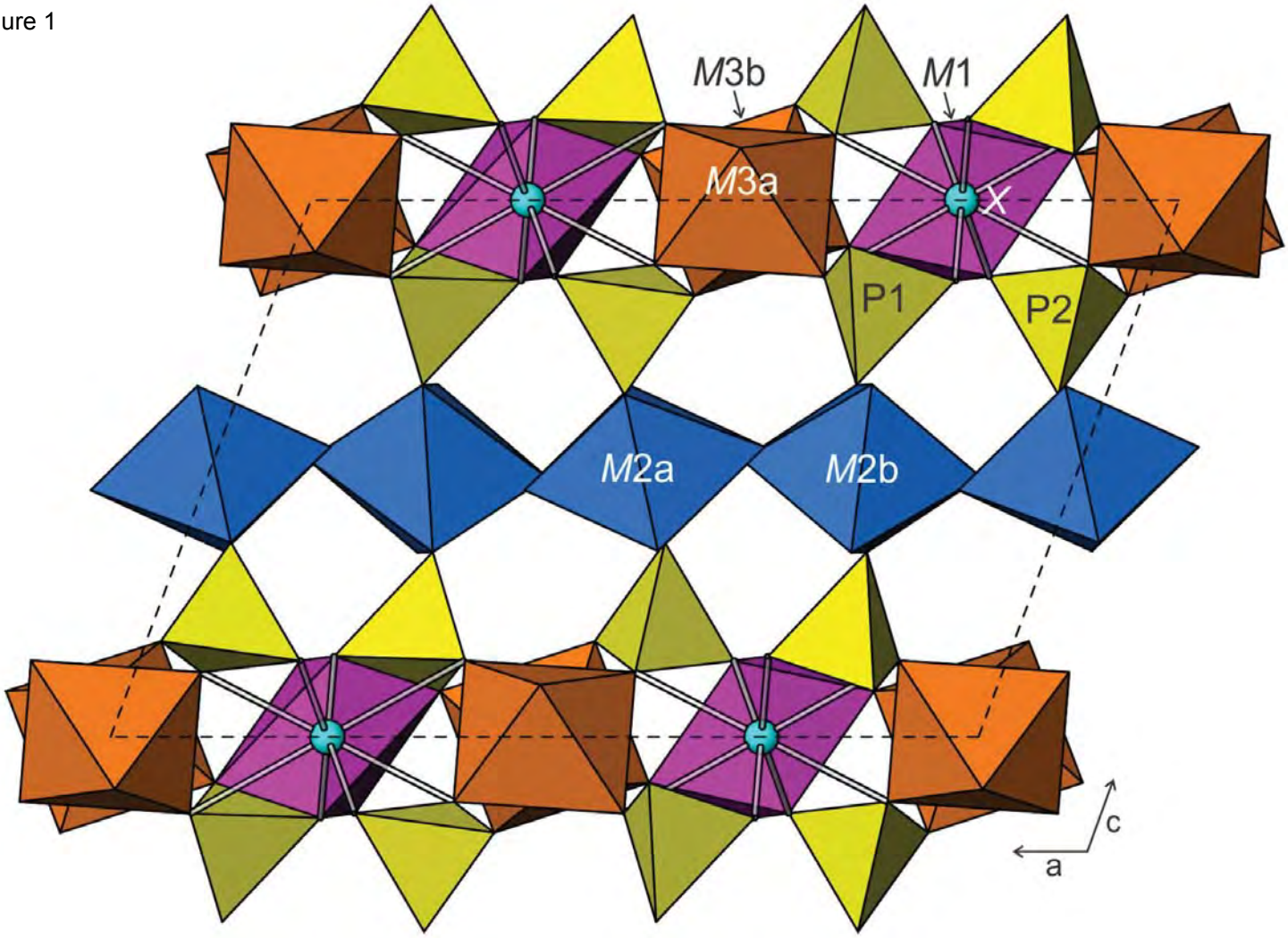

This is the peer-reviewed, final accepted version for American Mineralogist, published by the Mineralogical Society of America.
The published version is subject to change. Cite as Authors (Year) Title. American Mineralogist, in press.
DOI: https://doi.org/10.2138/am-2022-8174. http://www.minsocam.org/

Figure 2

This is the peer-reviewed, final accepted version for American Mineralogist, published by the Mineralogical Society of America.
The published version is subject to change. Cite as Authors (Year) Title. American Mineralogist, in press.
DOI: https://doi.org/10.2138/am-2022-8174. http://www.minsocam.org/

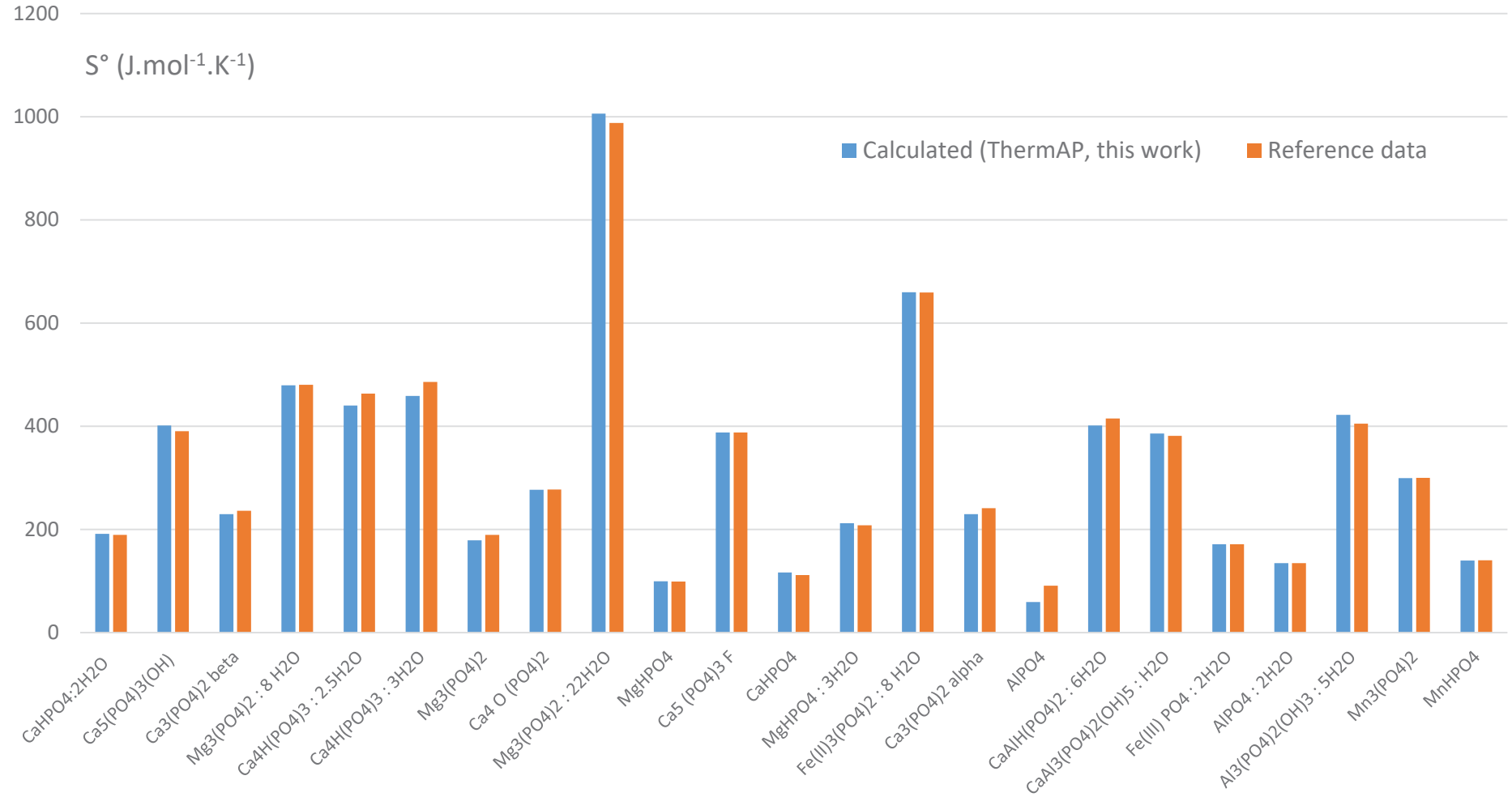

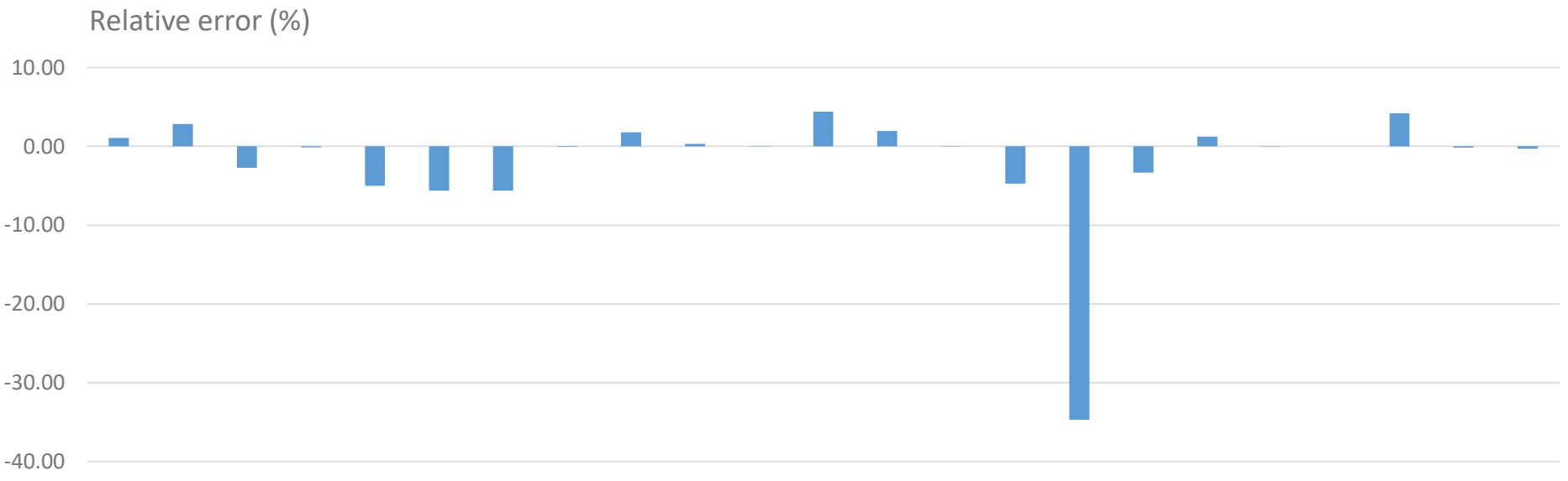

Figure 3

This is the peer-reviewed, final accepted version for American Mineralogist, published by the Mineralogical Society of America.
The published version is subject to change. Cite as Authors (Year) Title. American Mineralogist, in press.
DOI: https://doi.org/10.2138/am-2022-8174. http://www.minsocam.org/

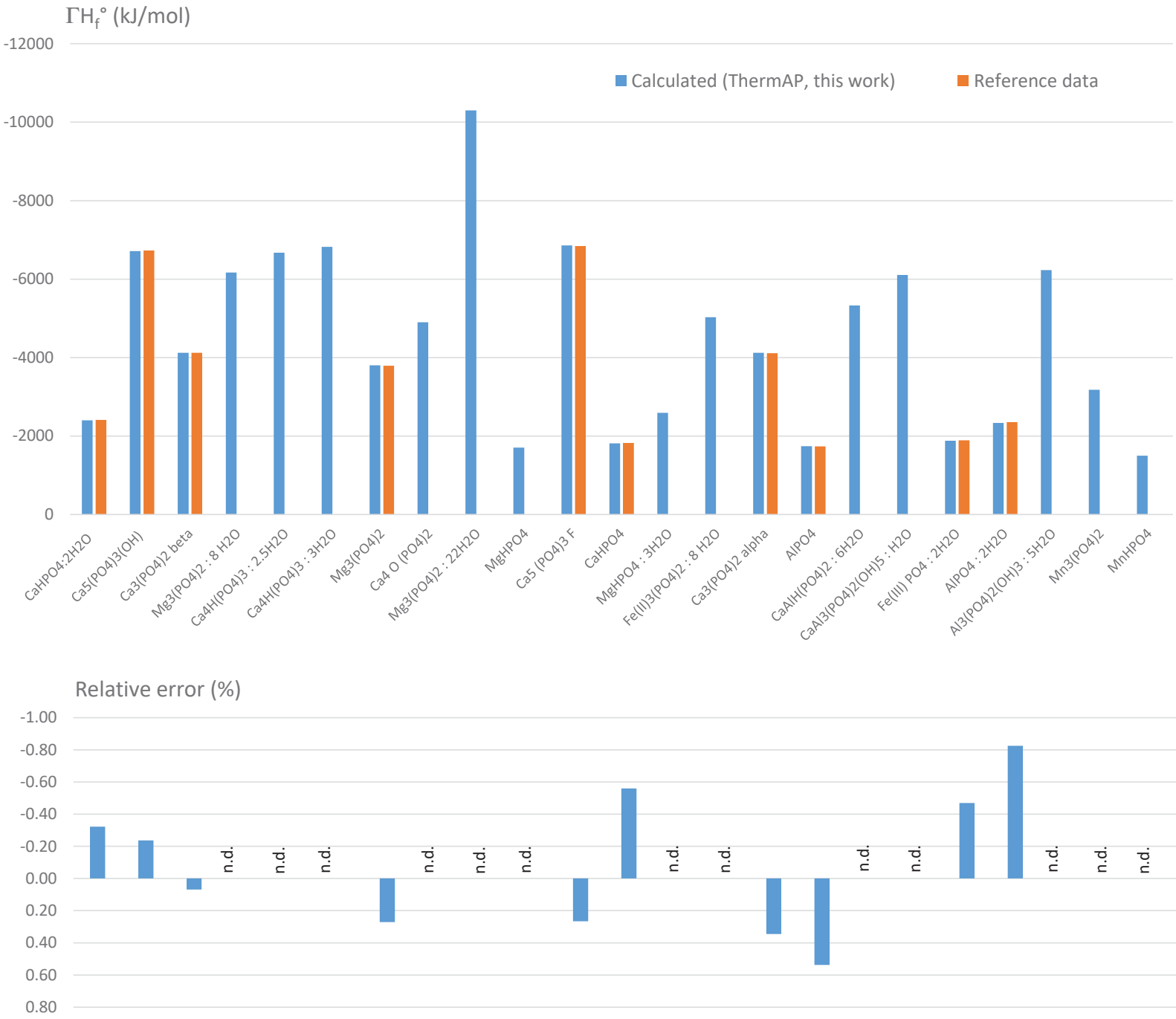

Figure 4

This is the peer-reviewed, final accepted version for American Mineralogist, published by the Mineralogical Society of America.
The published version is subject to change. Cite as Authors (Year) Title. American Mineralogist, in press.
DOI: https://doi.org/10.2138/am-2022-8174. http://www.minsocam.org/

Figure 5

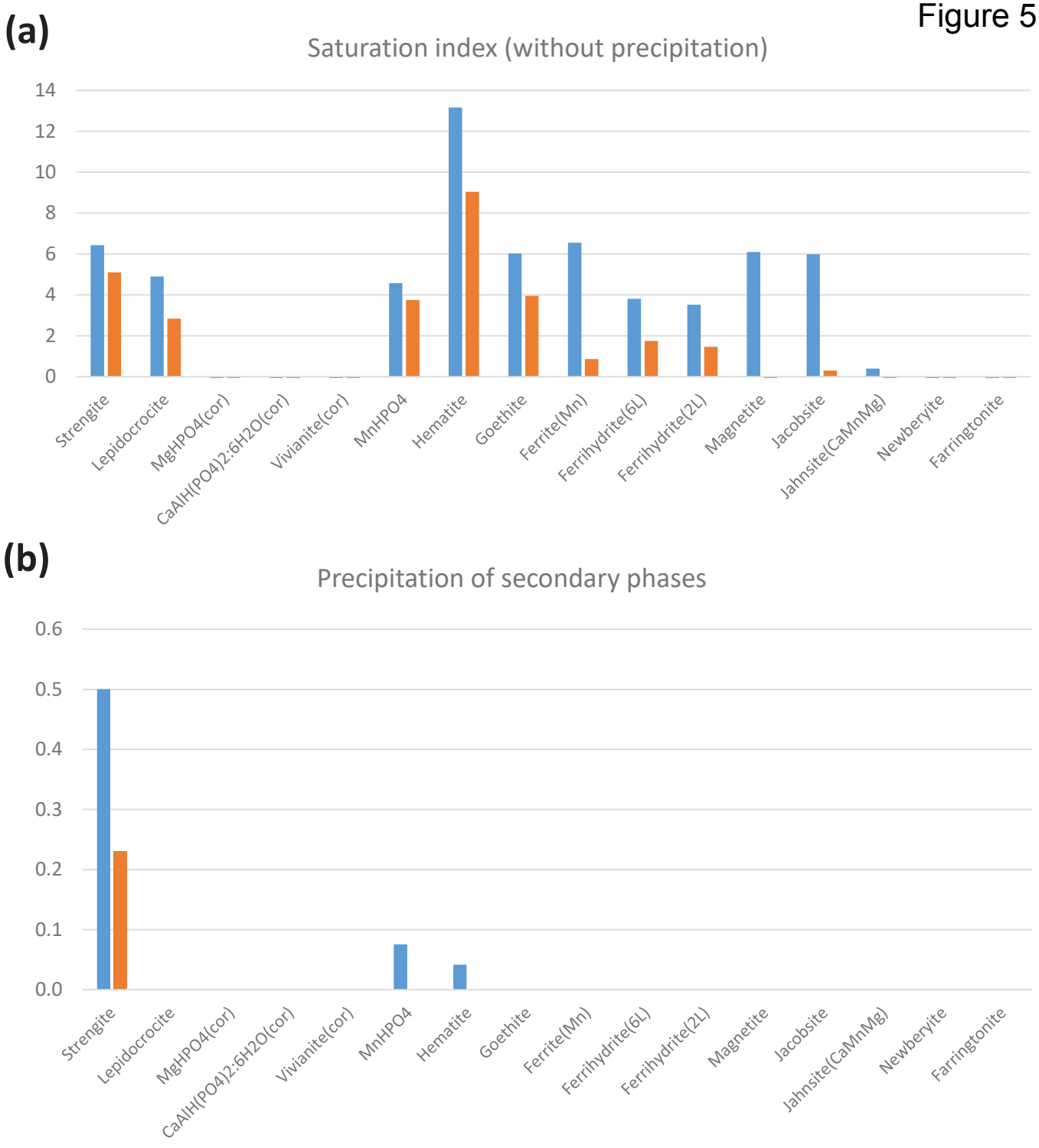

This is the peer-reviewed, final accepted version for American Mineralogist, published by the Mineralogical Society of America.
The published version is subject to change. Cite as Authors (Year) Title. American Mineralogist, in press.
DOI: https://doi.org/10.2138/am-2022-8174. http://www.minsocam.org/

Figure 6

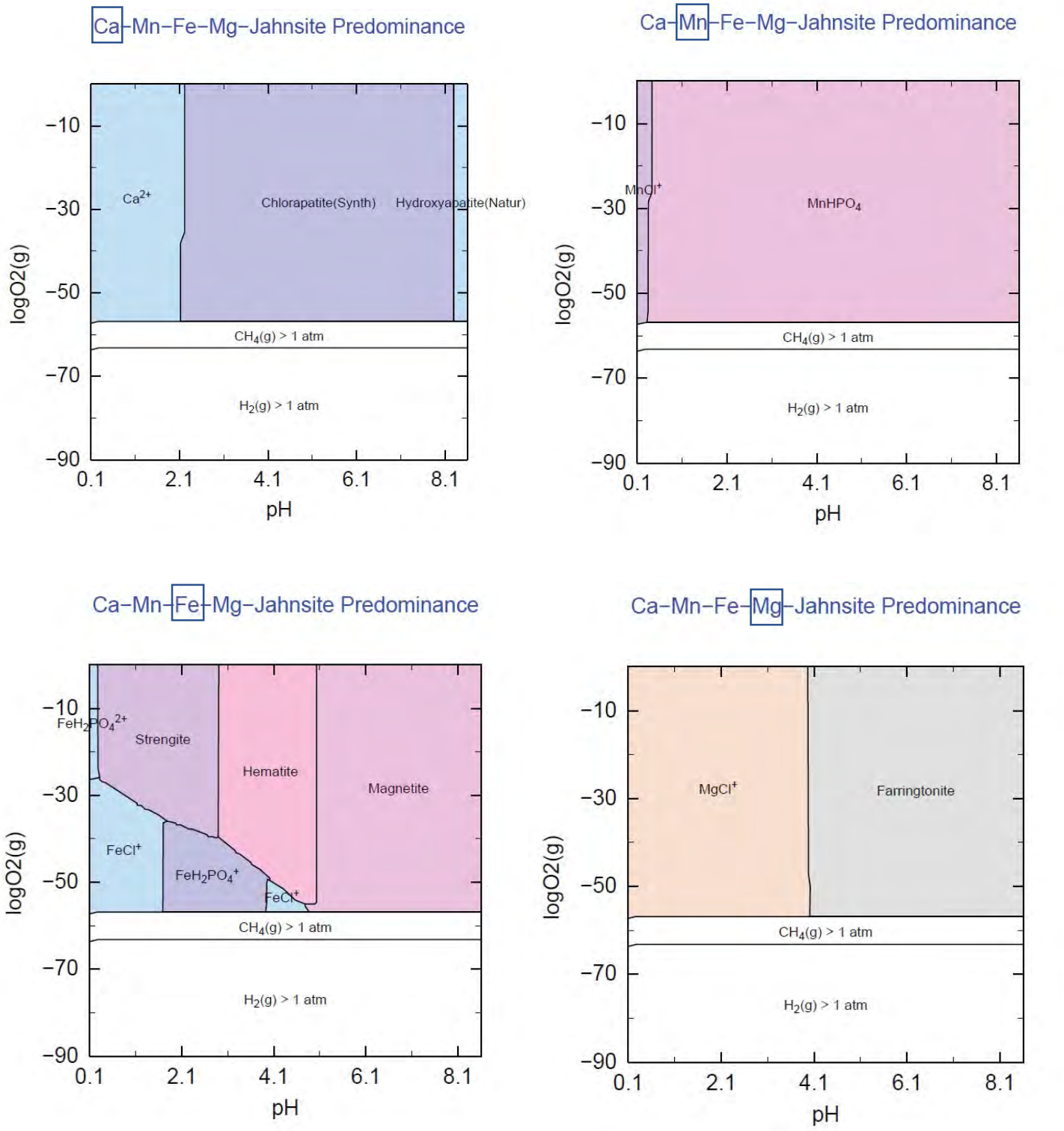

This is the peer-reviewed, final accepted version for American Mineralogist, published by the Mineralogical Society of America.
The published version is subject to change. Cite as Authors (Year) Title. American Mineralogist, in press.
DOI: https://doi.org/10.2138/am-2022-8174. http://www.minsocam.org/

Figure 7

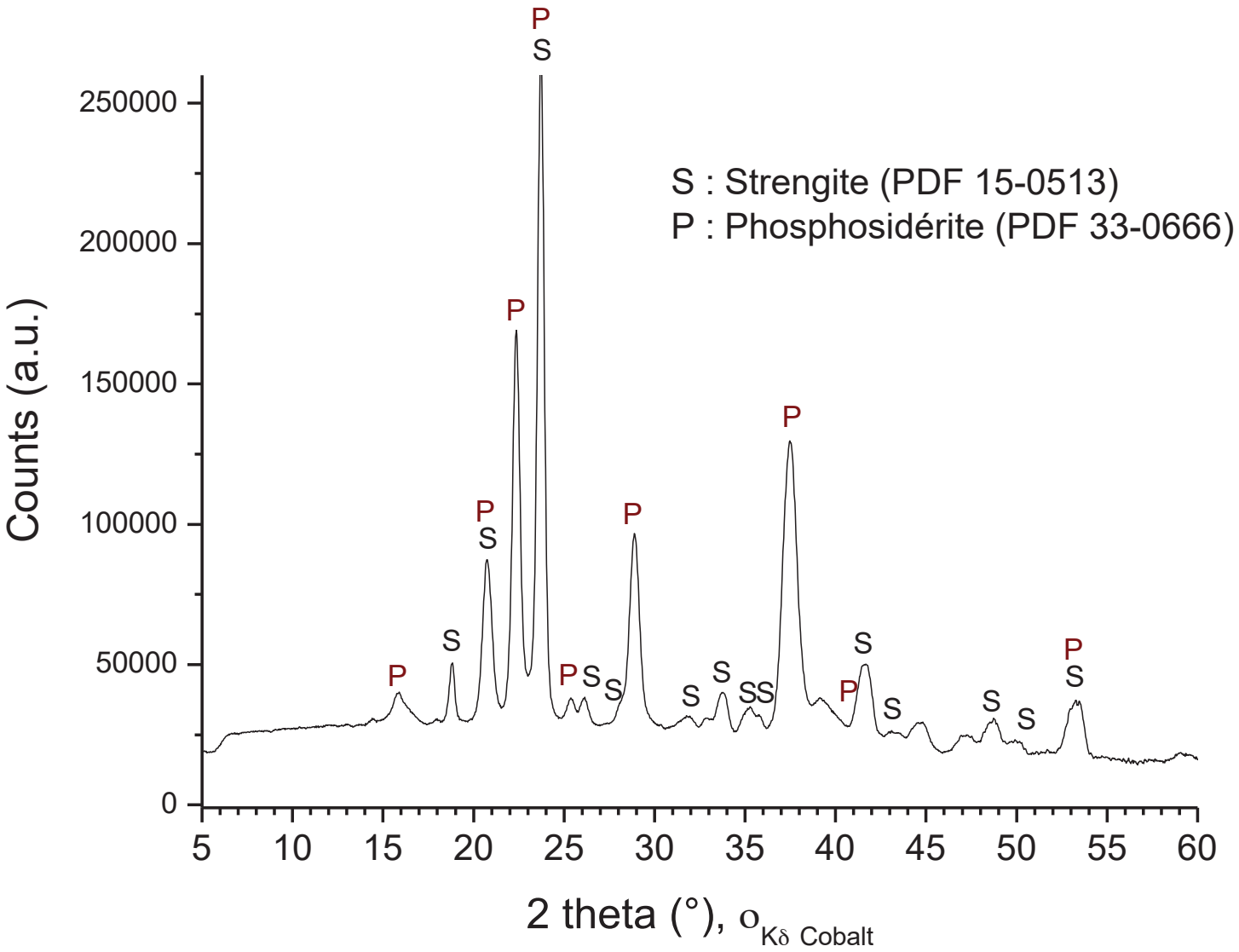

This is the peer-reviewed, final accepted version for American Mineralogist, published by the Mineralogical Society of America.
The published version is subject to change. Cite as Authors (Year) Title. American Mineralogist, in press.
DOI: https://doi.org/10.2138/am-2022-8174. http://www.minsocam.org/

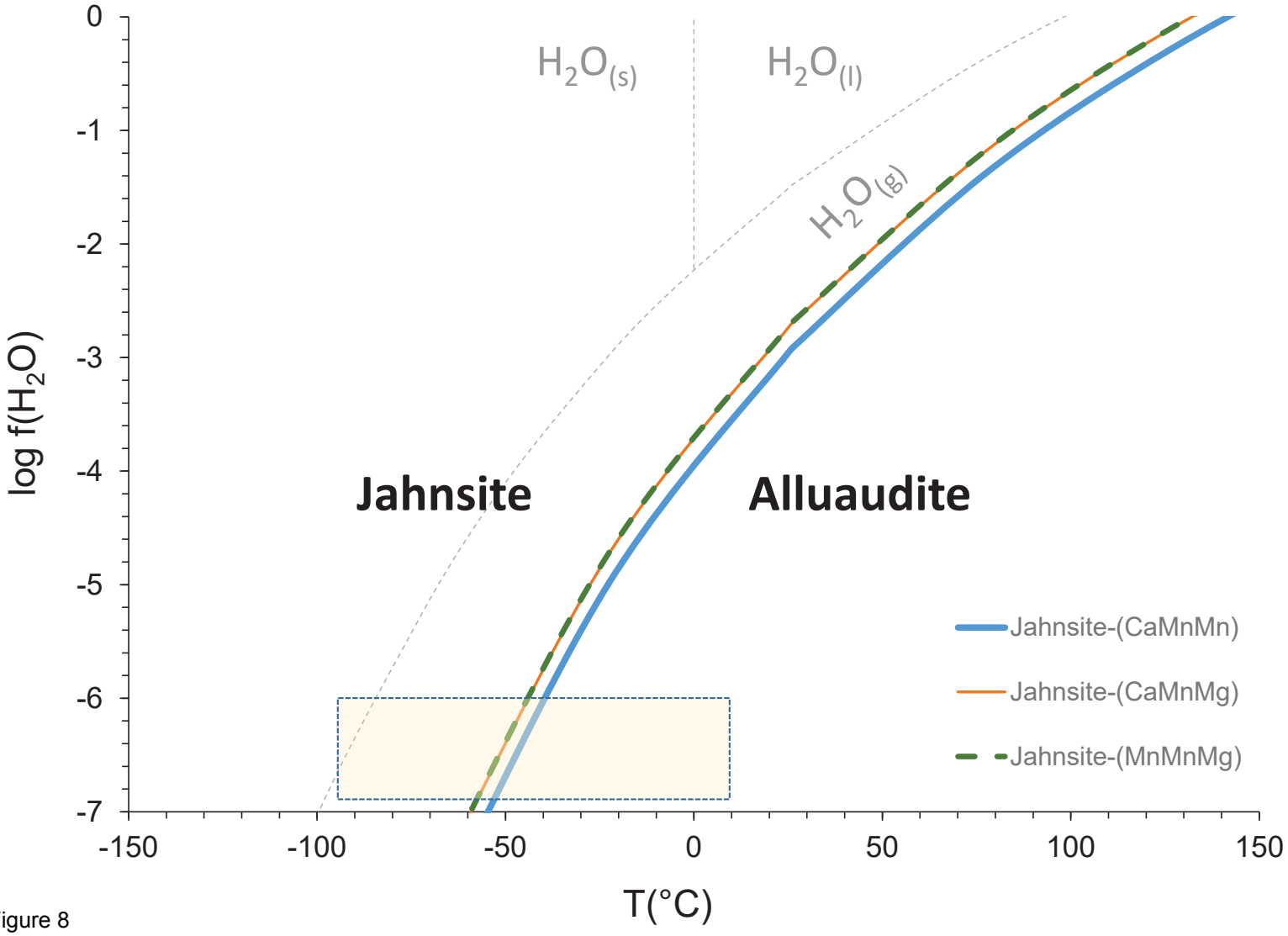

Figure 8